THE FLARES OF AUGUST 1972

HAROLD ZIRIN and KATSUO TANAKA
Big Bear Solar Observatory, Hale Observatories, Carnegie Institution of Washington, California Institute of Technology

(Received 9 April; in revised form 3 July, 1973)

Abstract. We present the analysis of observations of the August flares at Big Bear and Tel Aviv, involving monochromatic movies, magnetograms and spectra. In each flare the observations fit a model of particle acceleration in the chromosphere with emission produced by impact and by heating by the energetic electrons and protons. The region showed inverted polarity and high gradients from birth, and flares appear due to strong magnetic shears and gradients across the neutral line produced by sunspot motions. Post flare loops show a strong change from sheared, force-free fields parallel to potential-field-like loops, perpendicular to the neutral line above the surface.

We detected fast (5 s duration) small (1″) flashes in $\lambda 3835$ at the footpoints of flux loops in the August 2 impulsive flare at 18:38 UT, which may be explained by dumping of > 50 keV electrons accelerated in individual flux loops. The flashes show excellent time and intensity agreement with > 45 keV X-rays. In the less impulsive 20:00 UT flare a less impulsive wave of emission in $\lambda 3835$ moved with the separating footpoints. The thick target model of X-ray production gives a consistent model for X-ray, $\lambda 3835$ and microwave emission in the 18:38 UT event.

Spectra of the August 7 flare show emission 12 Å FWHM in flare kernels, but only 1 to 2 Å wide in the rest of the flare. The kernels thus produce most of the Hα emission. The total emission in Hα in the August 4 and August 7 flares was about 2×10^{30} erg. We belive this dependable value more accurate than previous larger estimates for great flares. The time dependence of total Hα emission agrees with radio and X-ray data much better than area measurements which depend on the weaker halo.

Absorption line spectra show a large (6 km/s^{-1}) photospheric velocity discontinuity across the neutral line, corresponding to sheared flow across that line.

1. Introduction

The active region McMath 11976, which produced the great flares of August 1972, produced an unparalleled opportunity for the study of solar activity. We present optical observations made at the Big Bear Solar Observatory and its station at Tel Aviv University, and comparisons with data kindly made available by various colleagues.

The data at Big Bear Lake were made with a battery of telescopes on a single mount. Two 10-in. refractors produced large scale cinematographic data in various wavelengths, mostly Hα and H$\alpha \pm \frac{1}{2}$Å, but also on August 2 with a Chapman filter (Chapman, 1971) 15 Å wide, centered on $\lambda 3835$. Observations of the full disc in Hα were made with an 8.6-in. vacuum refractor, white light full disc observations with a 6-in. refractor. Magnetograms were made with the Leighton-Smithson magnetograph (Smithson and Leighton, 1970), time sharing in one of the 10-in. refractors, and spectrograms, with the 5-m Coudé spectrograph fed by a third 10-in. refractor. At Tel Aviv, observations were made with a 5-in. photoheliograph used in the center of Hα. We were fortunate in that not only was the birth of the region observed in July, but all of the large flares were picked up on either the Big Bear or Tel Aviv photoheliographs. The principal large flares occurred at 03:30 UT August 2 (only observed

Solar Physics **32** (1973) 173–207. *All Rights Reserved*

in progress), 18:38 UT August 2, 20:05 UT August 2, 06:20 UT August 4, 15:16 UT August 7, and 12:16 UT August 11 (only late phases).

The highlights of the observations are the following: the region showed inverted polarity from its inception on July 11; the great activity was due to extremely high shear and gradients in the magnetic field, as well as a constant invasion of one polarity into the opposite; observations in $\lambda 3835$ show remarkable fast flashes in the impulsive flare of 18:38 UT on August 2 with lifetimes of 5s, which may be due to dumping of particles in the lower chromosphere; flare loops show evolutionary increases of their tilts to the neutral line in the flares of August 4 and 7; spectroscopic observations show red asymmetry and red shift of the Hα emission in the flash phase of the August 7 flare, as well as substantial velocity shear in the photosphere during the flare, somewhat like earthquake movement along a fault; finally the total Hα emission of the August 7 flare could be measured accurately as about 2.5×10^{30} erg, considerably less than coarser previous estimates for great flares. A preliminary report on our data has appeared (Tanaka and Zirin, 1973) and we present here our comprehensive analysis of the wealth of material obtained.

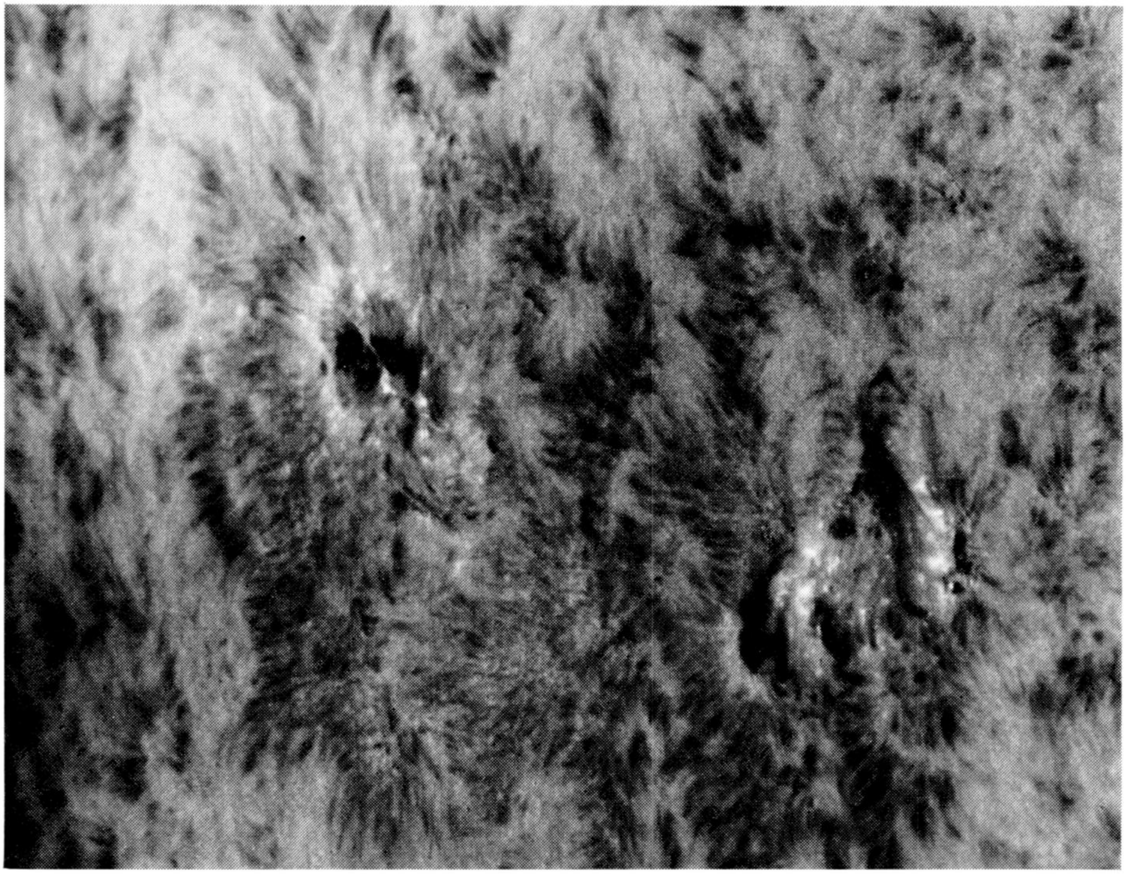

Fig. 1. Early stage of McMath 11976 (as McMath 11957) at 18:17:23 UT, July 12, Hα + 0.5 Å. It is in the lower right of the frame, a typical complex emerging flux region (EFR). The dark fibrils probably parallel new flux loops, and would normally run E-W in a simple region. Comparison with Figure 2 shows that the sunspot in the upper part of the group is *p* (preceding, or S) polarity, and the regions below and the surrounding are *f* (following, N). The spots at left died out on the back side of the Sun. *S top, W left on all photos.*

2. Development of the Region, July 10 to 15

McMath 11957, the predecessor of McMath 11976, first appeared on Big Bear films on July 11, growing in a quiet region. Figure 1 shows an Hα picture of development on July 12 and Figure 2, the magnetograms. In contrast to the conclusion of Bumba and Howard (1965) our unpublished data show that such regions do not emerge from the elements of the chromospheric network but at random. In this case the region emerged in a perfectly quiet area – note the black dot (*p* polarity) in the 10 July magnetogram. The magnetic polarity was inverted from the start, the arched filaments being rotated 120° from the normal E-W direction. In addition to the first set of flux loops, other

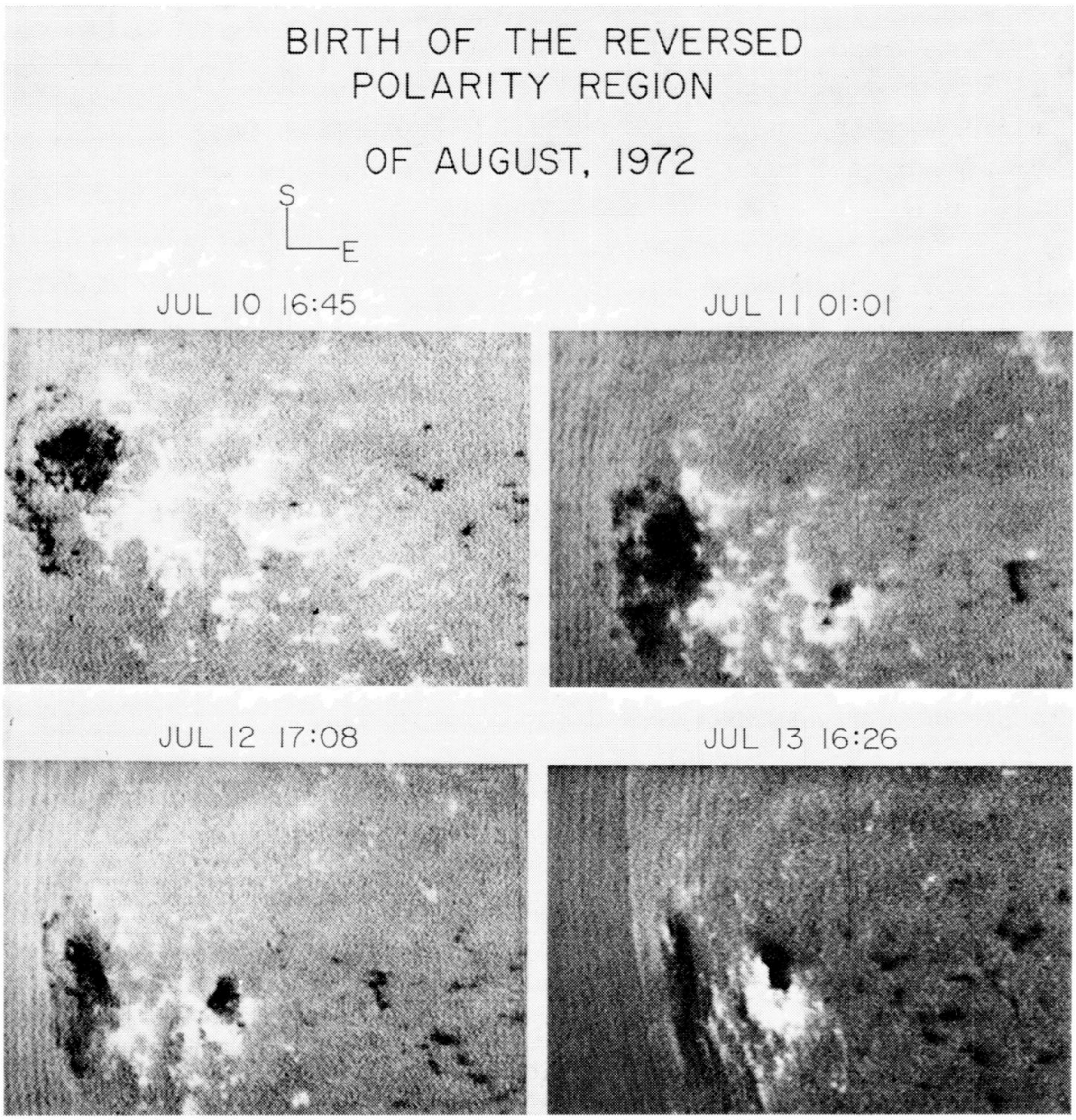

Fig. 2. A series of videomagnetograms of the birth of McMath 11957 made by James Mosher. Dark is *p* (preceding, or S in the northern hemisphere this cycle) polarity, white is *f* or following. Note the contrast of the complex new region with the larger old region at left, where dark (*p*) polarity leads, as it normally should.

systems arose, so that on July 12 there were 2 sets of *f* spots, both connected to the same *p* area. Between July 12 and July 13 there was rapid growth of the *p* spot, and the magnetogram for the 13th shows the strong field gradients thus produced. A number of small flares were observed in this region, and spectra were obtained of intense small surges at the limb on the 15th. The limb activity on the 15th was almost continuous, made up of many small surges. Although magnetic complexity often results from emergence of field in an existing region, the surrounding fields in this case were weak and do not appear to have played an important role. McMath 11947, the region just preceding, died out on the back side of the Sun.

3. Development July 30 to August 2

McMath 11976 appeared at the east limb on July 29, with high resolution observations at Big Bear beginning on the 30th. The region showed a tightly twisted magnetic configuration with steep field gradients and the normal polarities reversed. Such regions invariably give great flares. In Figure 3, we show an enlarged view of the spot on August 3 in Hα – 0.5 Å on which we have marked various features. Figures 4, 5 and 6 show the disk transit of the region from July 30 to August 11, and Figure 7 shows the daily magnetograms obtained by James Mosher. The region was only moderately active on the 30th and 31st of July; there were a number of small flares along the neutral line, all fast and impulsive. This neutral line, a sharp discontinuity between *p* and *f* longitudinal polarity, was the dominant feature of the group during its disc passage. Along it a ragged N-S line of field transition arches (FTA) (Prata, 1971; Zirin, 1972) and longer dark fibrils separated the *f* and *p* polarities. We distinguish these because the FTA in the upper part are short fibrils connecting nearby fields and running more or less perpendicular to the neutral line, whereas the fibrils in the lower (N) half, while physically similar, run, like filaments, parallel to the boundary line and are considerably longer. These long fibrils, which must follow the magnetic field lines, show the great shear that existed along the neutral line. Eventually the FTA were sheared into filaments, and filament 1 extended, with a few breaks, all the way through the group.

The spot p_1, in particular, which seems to have produced most of the activity, was connected to f_2, whereas a much shorter, lower energy connection to the near part of f_3 was possible. The large p plage pl_1, enclosed by the filament *fil 1*, which did not form completely till August 1, was sharply bounded on the left (west) by the filament, with horizontal polarity only a few thousand kilometers away. Note that the neutral line was almost N-S on August 1 and became sharply kinked afterwards.

The spot p_1 was indeed remarkable, and more so as it grew. It shows normal longitudinal spot polarity in the magnetogram, but the overlying Hα fibrils show transverse field a few thousand kilometers above, so the field makes a sharp turn. Because the spot grew so rapidly it must be half of an emerging flux region (Zirin, 1971), and indeed it was connected to f_3, which moved eastward while p_1 plowed into the flux ahead in the normal expansion of an emerging flux loop. The two spots are seen

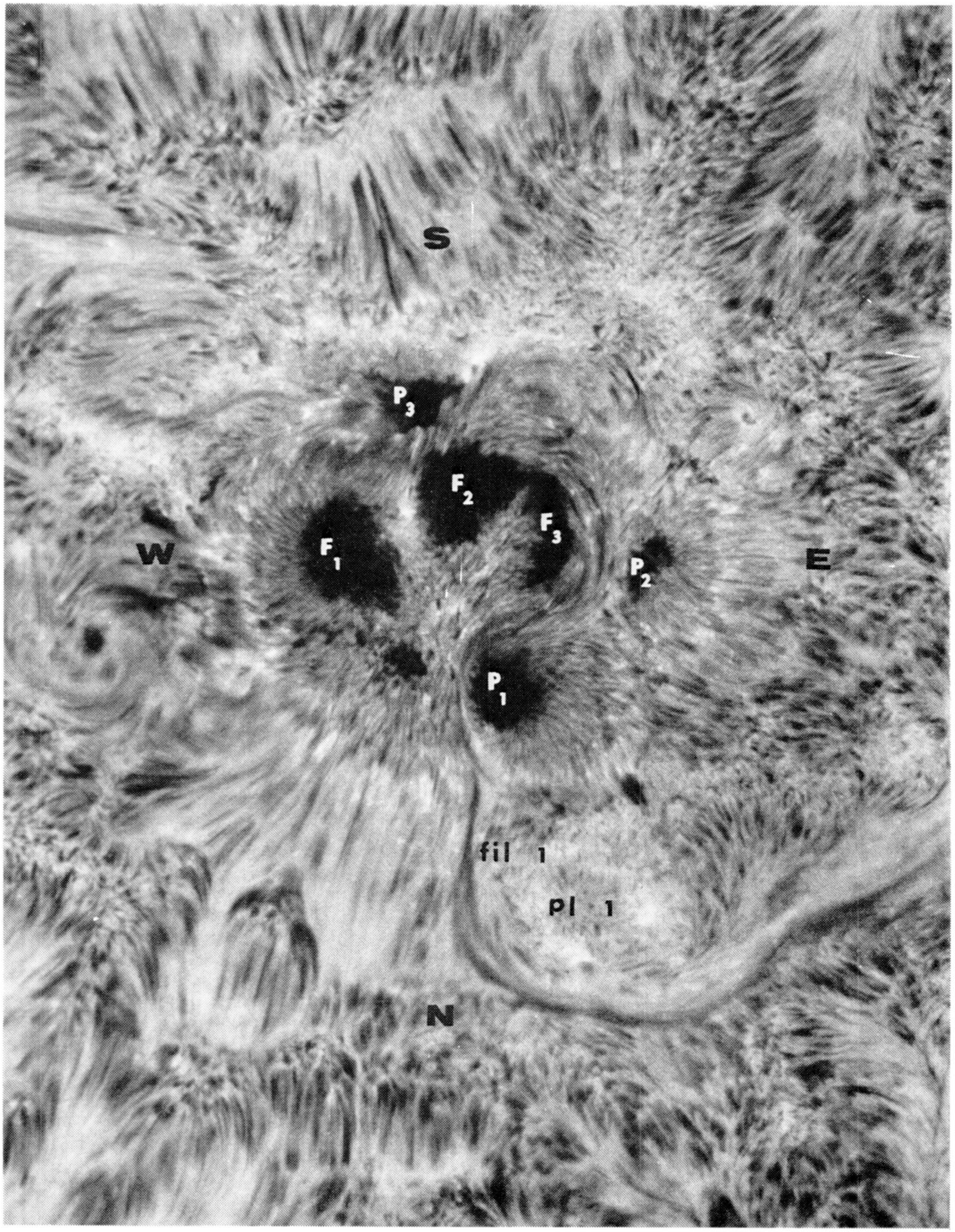

Fig. 3. An enlarged frame 8/3, with various sunspots and areas marked to facilitate reference in the text. Note the strongly twisted penumbral structures.

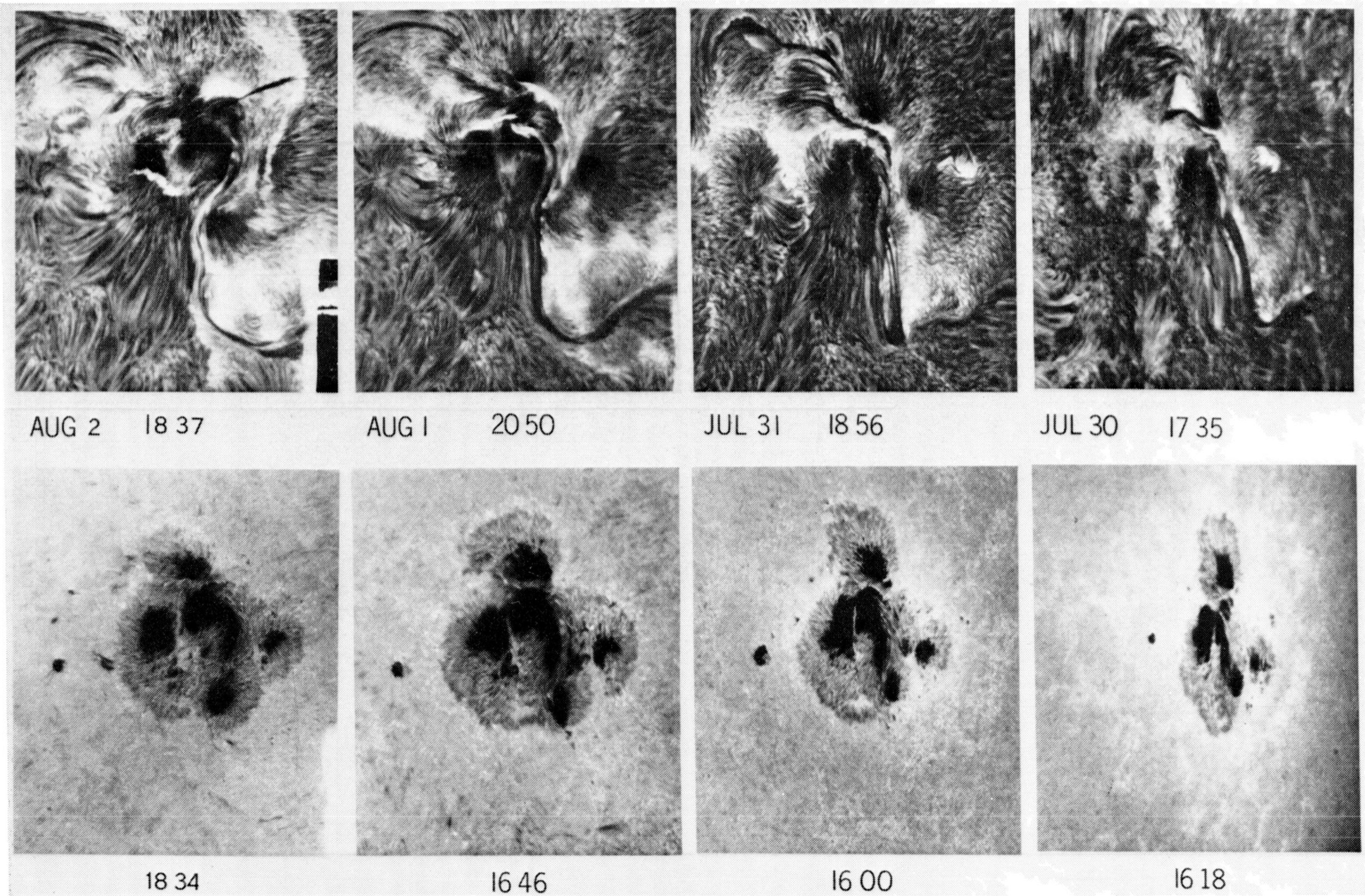

Fig. 4. Synoptic series 7/30–8/2, with Hα centerline, best for plages and filaments, above, and H$\alpha - 1.0$ Å, best for sunspots, below. Note the rapid growth of the lower spot, designated p_1, and the increase of twist in the neutral line between p_1 and f_3.

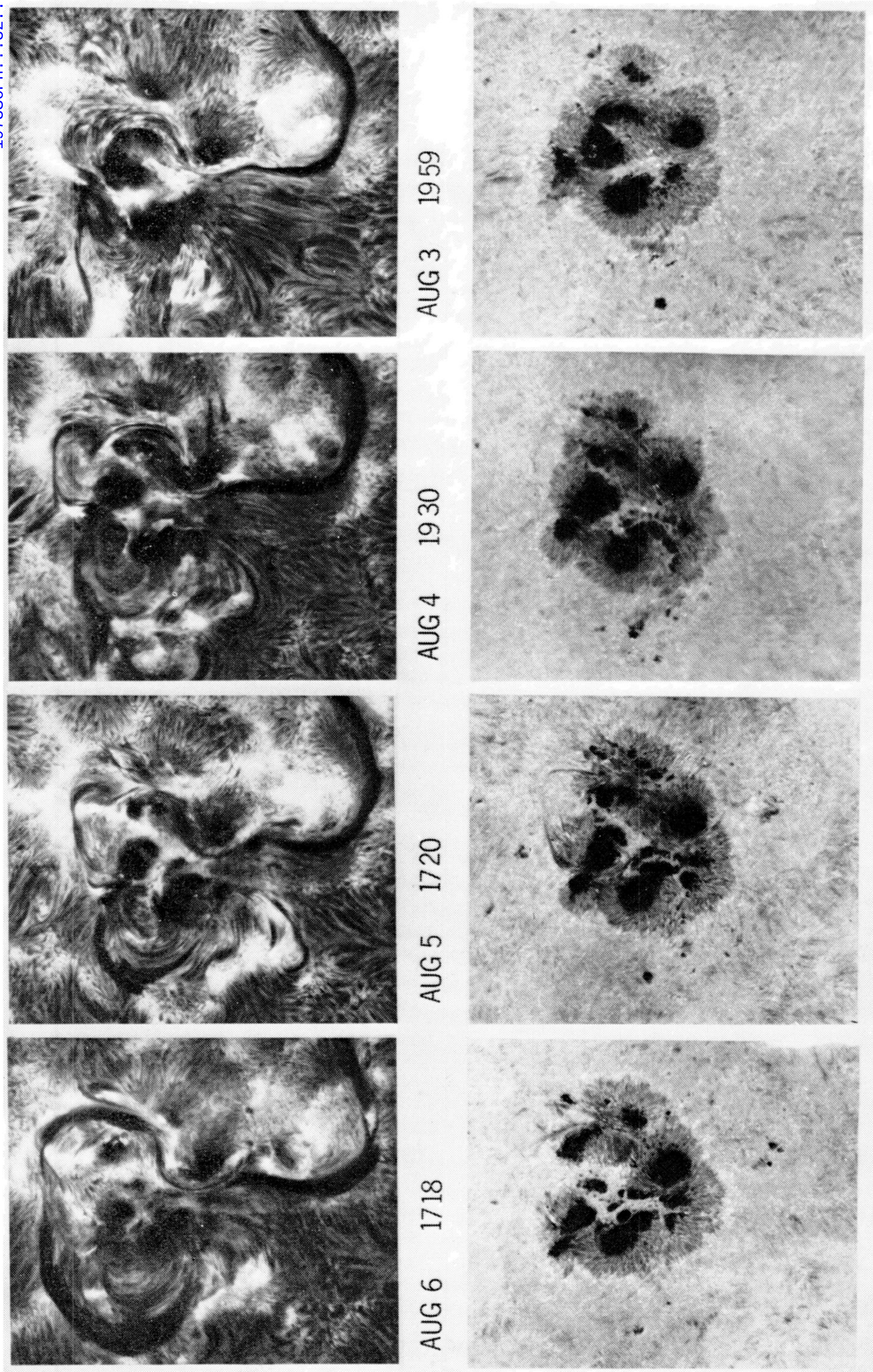

Fig. 5. Further development, 8/3–8/6. Note the filament development and the E-W separation of the p spots. Note also the further increase of shear in the neutral line between p_1 and f_3. On 8/6 a complex double ring exists around f_3 in the main flare area.

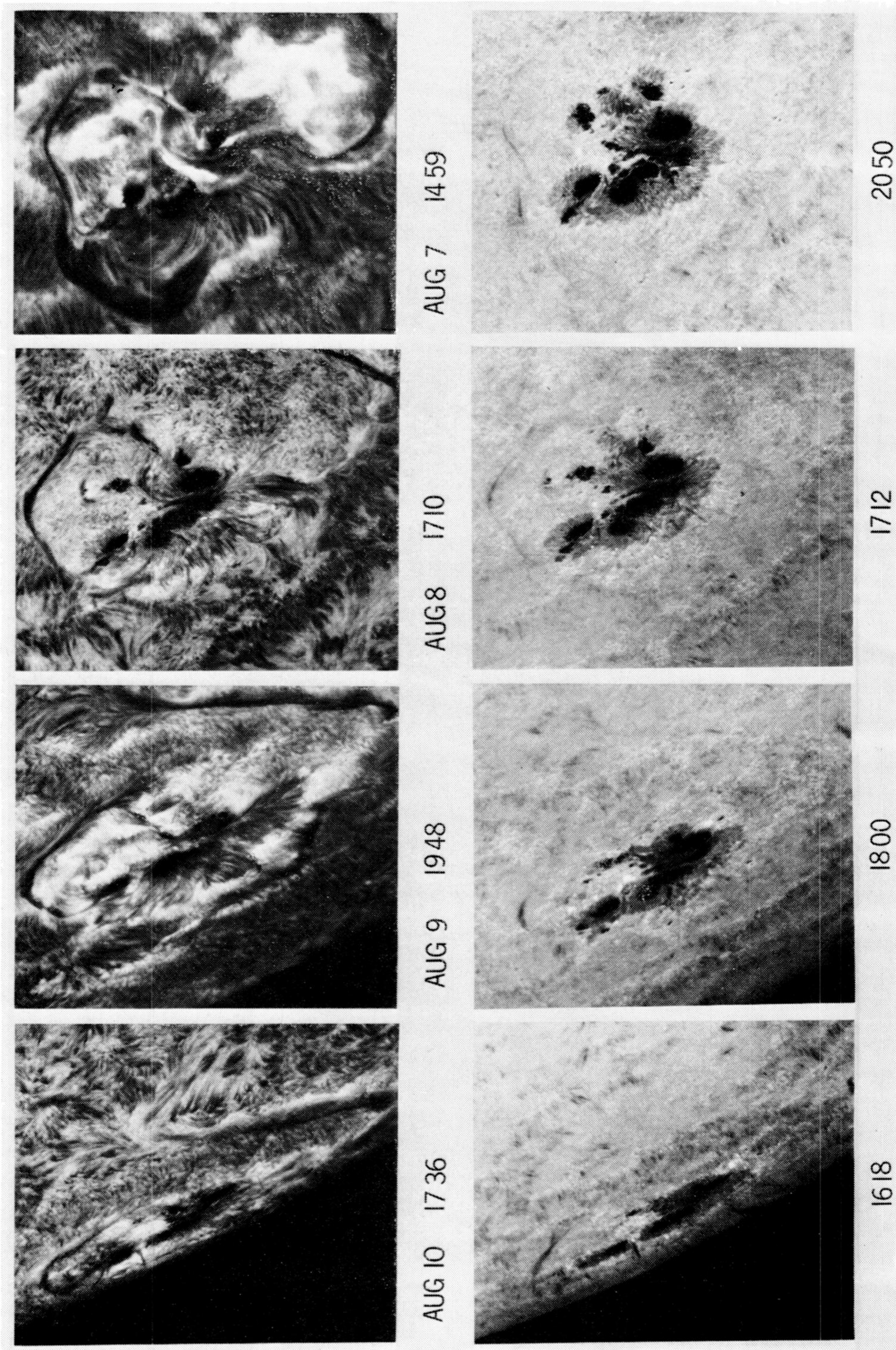

Fig. 6. Development 8/7–8/11. The region simplified after the 8/7 flare. The 8/10 frames show how shallow is the vertical structure. Two pictures (August 8 and August 10, upper) are taken at −0.5 Å.

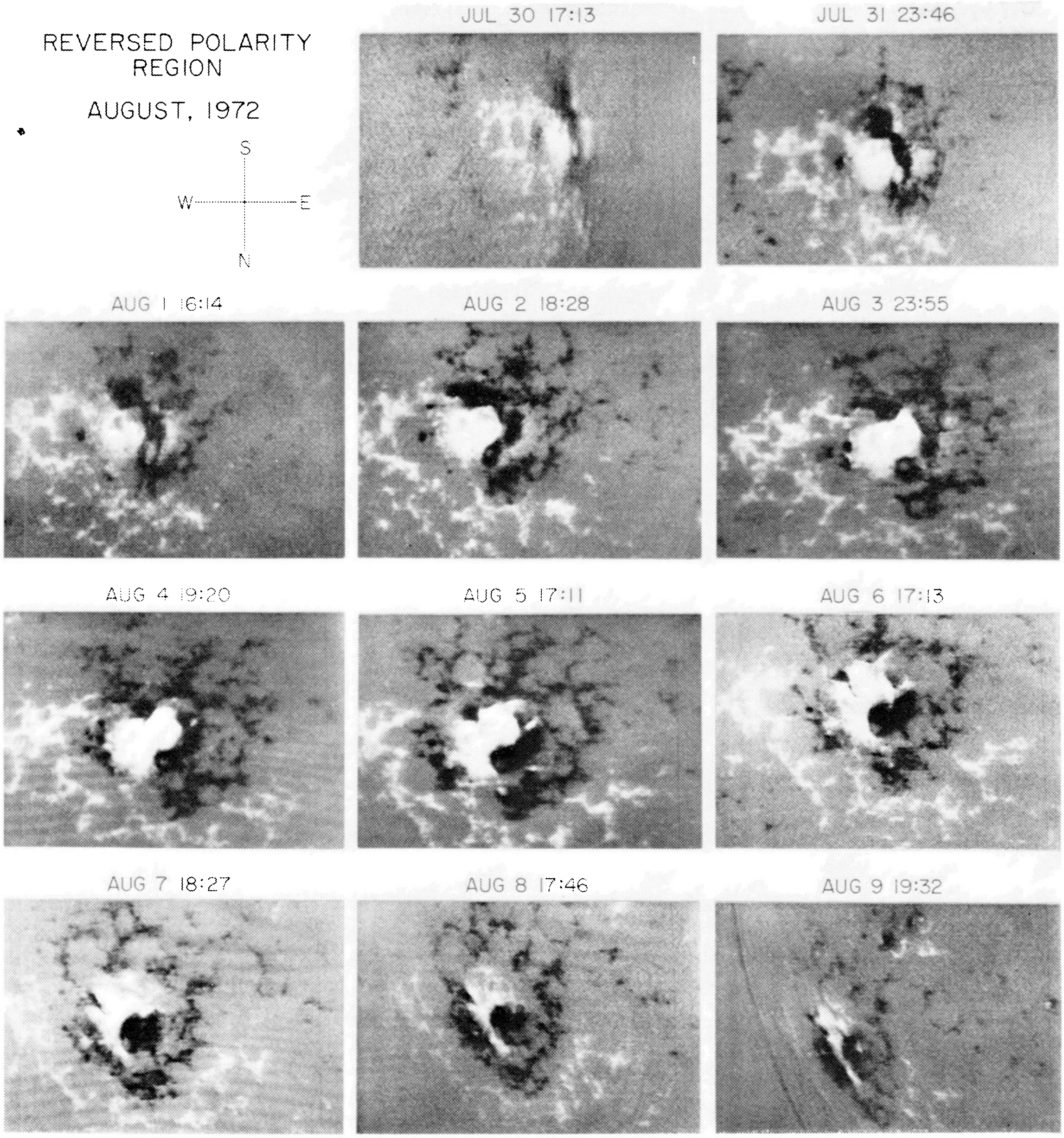

Fig. 7 Videomagnetograms for 7/30–8/9. In this series white is following (f) polarity, dark preceding; the intensity of light or dark shading is proportional to the longitudinal field strength. The growth of spot p_1 is clearly seen as intense dark polarity below, and the eastward spread of f_3 is seen as the rightward spread of white polarity. Very rarely do such strong gradients appear.

to be connected by dark fibrils which are bright and active at both ends. Several flares are bright at both points. But these fibrils, in contrast to the normal arched filament systems, are strongly twisted and not prominent in pictures off the center of Hα.

A particular feature of this group was the sharp twisting of penumbral fibrils seen in white light pictures and in Hα off-band pictures as well, to run parallel to the neutral line. Such a twisting means that the sunspot field, which normally falls off like $1/r^2$, as the penumbral fibrils radiate outward, is confined to a narrow corridor of sheared fibrils, and the horizontal field in this corridor may reach spot values (i.e.

2000 G or more). This feature of sheared penumbras (i.e. the side of the spot facing the neutral line has the penumbra sheared off) is common in regions giving big flares (e.g. August 28, 1966, Zirin and Lackner, 1969).

On August 1 there were continual bright flashes along the neutral line, and by the end of the day, two areas at opposite ends of the neutral line, near f_2 and p_1, were growing steadily brighter. The spot p_1 was completely covered by horizontal fibril structure. These fibrils go south from p_1, and, crossing above p_1 are fibrils going N from f_3. Since the fibrils must lie along the field lines, there were at least two polarity reversals above p_1, which of course must have longitudinal polarity. Fibril crossings of this type seem to be common before flares (Lazareff and Zirin, 1973; Zirin, 1973).

4. Flares of August 2

Major activity began in the region on August 2 with a remarkable series of complex flares. The first great flare was reported at 03:16 UT by Teheran; the later phases or perhaps a resurgence (two flares were reported but only one radio burst) are visible on our Tel Aviv photograph of 05:43 UT (Figure 8). This shows a large flare with bright strands covering all the spots, the brightest portion being over p_2. It differed from the later flares in that the f emission was confined to the spots and an area directed west. The long, dark filament following the group had disappeared, blown away by the flare. It reformed in bits and pieces, was blown away again by the later flares,

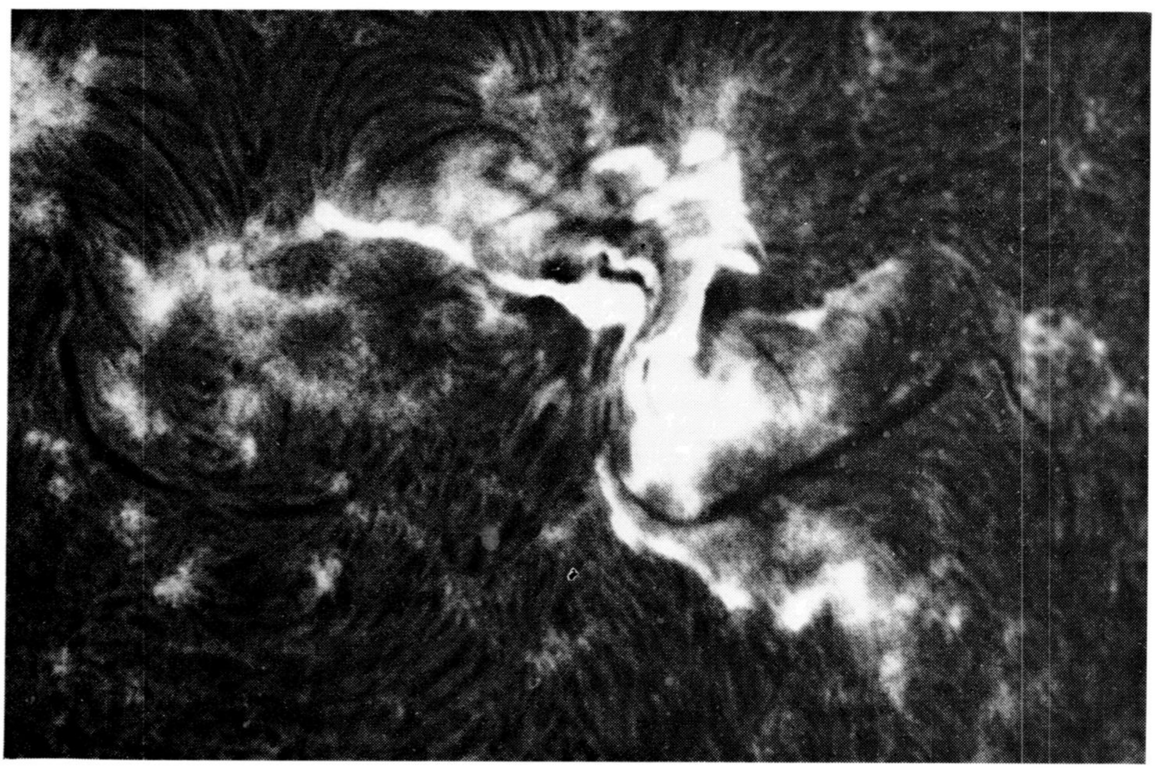

Fig. 8. First flare, August 2, photographed at Tel Aviv, dawn, by Shlomo Hoory in Hα centerline. This photo at 05:43:38 UT, more than two hours after the flare began, shows that it was similar to the later great flare.

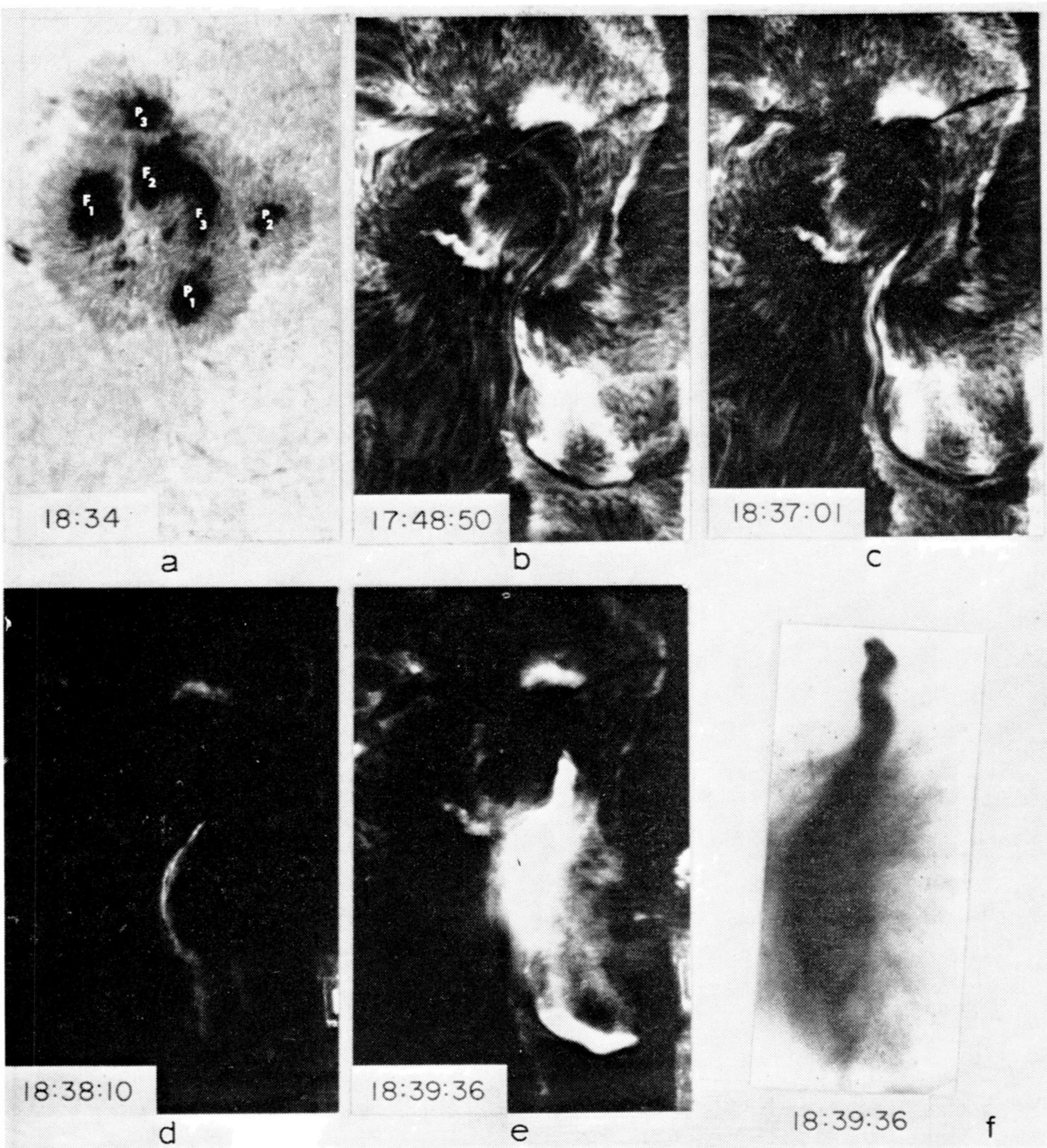

Fig. 9. A series of prints made to show varied aspects of the 18:38 UT flare (18:34 UT) Hα + 1 Å, showing spot structure, with spots marked. Note that all the spots lie in one penumbra, and the umbrae and penumbrae of p_1 and f_3 are twisted to follow the horizontal lines of force, rather than the normally radial structure.

(17:48:50 UT) – Hα before the flare. Note that the filament is sharp.
(18:37:01 UT) – The filament begins to break up into shorter fibrils.
(18:38:10 UT) – Dark print of flare beginning.
(18:39:36 UT) – Brilliant halo around the flare, probably Hα scattered by surrounding chromosphere.
(18:39:36 UT) – Light negative print, heavily dodged to show the structure of the flare kernel. Note that this picture is enlarged by a factor of two.

and was whole again on August 3. By contrast, the great flares of August 4 and 7 only made it wave about. Whether or not the flare was associated with changes in the magnetic field structure, there were definite changes on the 1st and 2nd; the spot p_1 grew, and the spots p_2 and p_3 shrank, so that at August 2, 16:00 UT, p_1 was bigger than the other two (eventually p_1 became the largest spot in the group). Spot p_1 also pushed ahead (W) relative to the other spots, as can be readily seen from the illustration (Figures 4 and 5); by August 2nd, the neutral line marked by the filament was directly beneath (N) of the *f* spots. A remarkable change also occurred in the fibril structure preceding the spot p_3. On the 31st, this was directly above (S) of f_1 and very close to p_3, almost along the neutral line dividing f_1 and p_3; on the 2nd (after the first flare), the fibril on the neutral line had moved considerably ahead (W) of p_3 and a new fibril system connected p_3 to f_1, with p_3 rapidly decaying. We have suggested before (Zirin, 1973) that a sheared neutral line can be replaced by shorter lines going directly across the neutral line to the nearest opposite polarity; this appears to occur in this case. The flux in p_3 can disappear by shortening and eventual subsidence below the surface of the flux loops. The energy released in this flare would presumably be the difference between the elongated sheared lines and the shorter field lines of the final configuration. This difference was actually observed during later flares; for example, in the flare 18:38 UT, August 2, a rapid break-up of the filament into shorter fibrils occurred at 18:37 UT, one minute before the brightening started (Figure 9). For the flares of August 4 and August 7, we could see the bright flare loops cross the neutral line with increasing tilts, late in the flash phases (Figures 18 and 19). If there is a further contraction involved in the subsidence of field lines below the surface, this energy too is available for the flare. In succeeding days p_3 moved considerably closer to f_1 and thus lowered the total energy.

On August 2, Big Bear observations were made in Hα centerline and λ3835. After a small flare along the neutral line at 16:01 UT, a brilliant impulsive flare began at 18:38 UT. Its development is shown in dark prints in Figure 9 and in normal prints in Figures 11a and 11b. The flare occurred along the neutral line between p_1 and f_3 following a break-up of fibrils on the neutral line (Figure 9, 18:37 UT) and spread rapidly along that line; there was a fast increase at 18:39:02 UT and another rise to a peak at 18:39:36 UT; these coincide with an early hard X-ray peak at 18:39:00–10 UT and a main peak at 18:39:30–40 UT. The dark prints, Figures 9d and 9e, and the negative print, Figure 9f, show the structure of the kernel. (The kernel consists of chains of bright points along the neutral line with an area of 3.8×10^{17}cm^2 and a diffuse halo with an area of 2.1×10^{18}cm^2.) This was the most brilliant flare we have yet seen in Hα, although its limited area kept the total fluxes down. This was not a classic two-ribbon flare; however, in the late phase (18:45 UT) two emission strands were seen displaced along the neutral line, confined in the inner edges of p_1 and f_3. At 18:41 UT fast ejection of material was observed along the neutral line to the north of p_1.

Figure 10 shows how a sequence of brilliant fast flashes along the neutral line occurred in λ3835. They occurred precisely at the W edge of umbra p_1 and the E edge

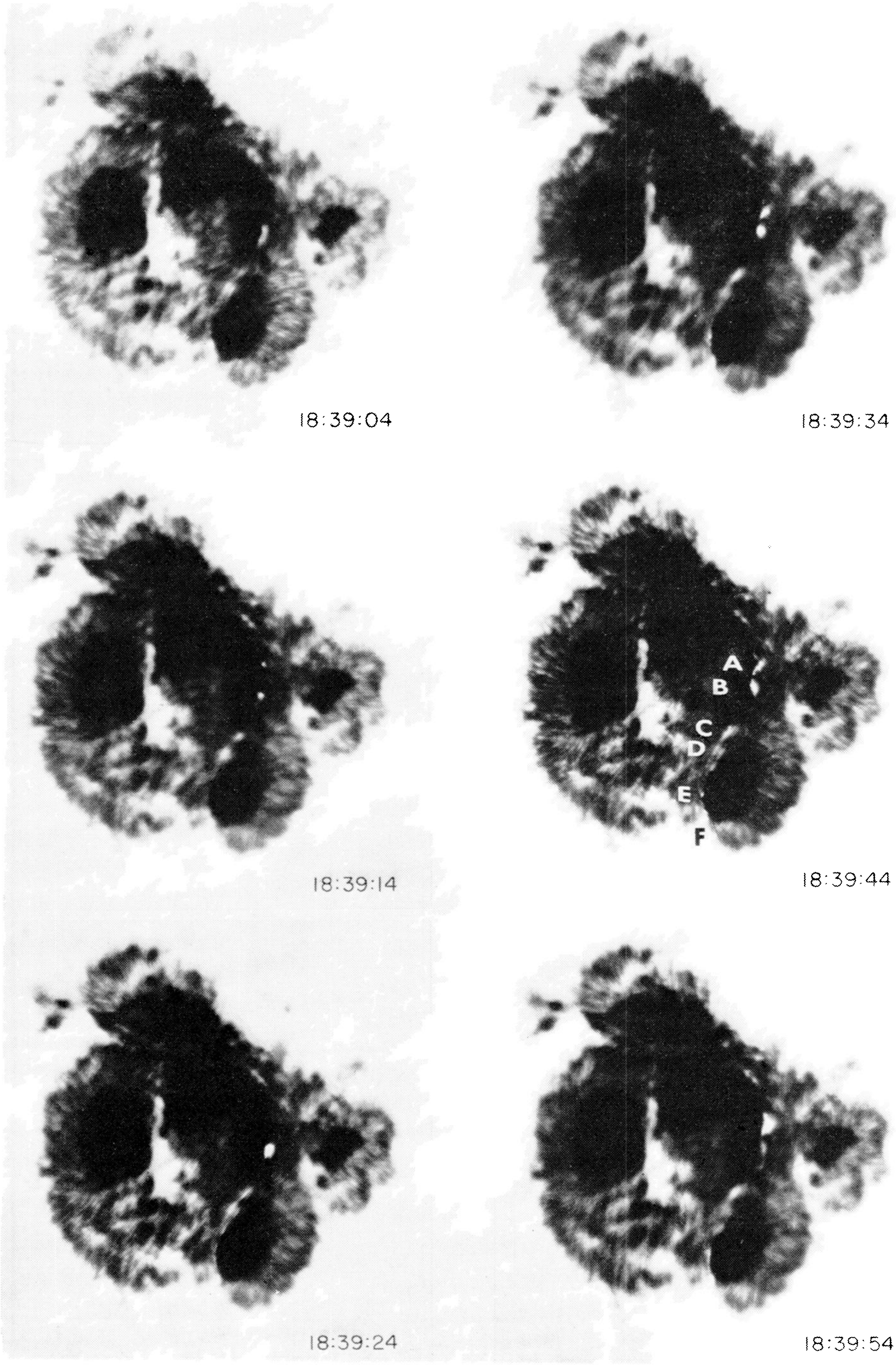

Fig. 10. Dark prints showing the flashes in 15 Å band centered at λ3835. The two bright strands at D (18:39:44 UT and earlier frames) mark the neutral line; flashes above this are in *f* polarity, below in *p* polarity. The two bright strands on the left edge of the spot coincide with the Hα maximum. All flashes occur precisely at the edge of the umbras, where the field lines turn and intersect the surface. These pictures are taken with a corrector designed by the late Professor I.S. Bowen to remove the aberration of the singlet lens; unfortunately it was not properly adjusted and there is some astigmatism.

of umbra f_3, showing how close to the edge of the umbrae the field became horizontal flashes above either umbra or penumbra would probably have been visible, but were not seen. The average lifetime of the points was 5 to 10s (frame rate was 5s) and their individual size can be seen to be less than 1″, although some appeared in groups and had larger area (for example Figure 10 (A), (B) and (C) at 18:39:44 UT). The double bright strands (D) in Figure 10 mark the Hα center, and presumably corresponds to the usual *p* and *f* polarity strands, but are much closer. The strands (D) and point (B) rose with the first X-ray pulse, then broke up into faint points; a new bright point appeared at 18:39:24 UT ,as the flux rose. It faded in 10s, and a row of points flashed into view at the X-ray maximum, 18:39:34 UT. The points appeared in symmetric pairs such as points (A) and (E) at 18:39:44 UT, points (A) and (F) at 18:39:54 UT, points (B) and (D) at 18:39:04 UT, points (B) and points between (E) and (F) at 18:39:24 UT; the lower points are less visible. As time passed, more points appeared to the north edge of p_1. By 18:40:00 UT, no more flashes were seen except for the lingering of point (F), which was under a long-lived Hα flare knot.

We interpret the λ3835 flashes as occurring at the intersection of flux loops with the surface; the emission must be due to the heating of the lower atmosphere by energetic electrons as they are accelerated in individual flux tubes and give up their energy at the surface. Thermal conduction from the flare above as an alternative source of heating would not be able to explain the fast time variation and limited extent of the flashes; the collision frequency at these densities is sufficient to produce conductivity across the field line which would rapidly homogenize the temperature in the source region, making difficult selective and time-dependent heating of the lower atmosphere, as well as spreading the emision area. Detailed discussions of the λ3835 flashes related to the X-ray and radio bursts will be given in the next section.

The activity of August 2 was not yet over; more flares were to come. Although the filament *fil 1* was disrupted, it reformed and straightened again; bright areas resulting from the flare remained, particularly of the *E* edge of *fil 1*. At 19:57 UT the area below spot p_1 brightened slowly, then more rapidly after 20:01 UT (Figure 11c). A weak brightening in λ3835 appeared at the most intense portion of the Hα flare. This flare reached maximum around 20:05 UT and remained stable; it produced a modest hard X-ray burst, but little radio emission; at 20:20 UT a new increase in area and brightness began on both sides of *fil 1* and at 20:30 UT yet another wave of brightening spread south from *fil 1*; this was matched by a bright region (Figure 12) in λ3835 (twice the photospheric intensity) just at the edge of the advancing bright Hα front. At the same time the entire *p* side of *fil 1* brightened as well. The λ3835 emission in this flare was not impulsive at all, lasting more than 15 min, although the lifetime at any point on the surface was only a few minutes. Again it appears to mark the footpoints of flux loops containing the energetic material (this time thermal conduction can be the heat source). The hard X-ray flux increased again and a large 6600 sfu, 8800 MHz burst occurred. The Hα front spread steadily on to a maximum at 20:50 UT (Figure 11d); the λ3835 emission moved south with a constant velocity of 12 km s^{-1} and changed its direction to northeast when it hit the edge of penumbra

p_1 as if it was reflected by the spot field. The λ3835 emission could be followed till 21:05 UT, but by now the Hα emission near the filament was dying out and the whole flare faded, accompanied by fine dark loops. But the last bright parts of this flare, spreading over f_2 and p_1 (Figure 11e, f), produced at 21:40 UT the greatest peaks of

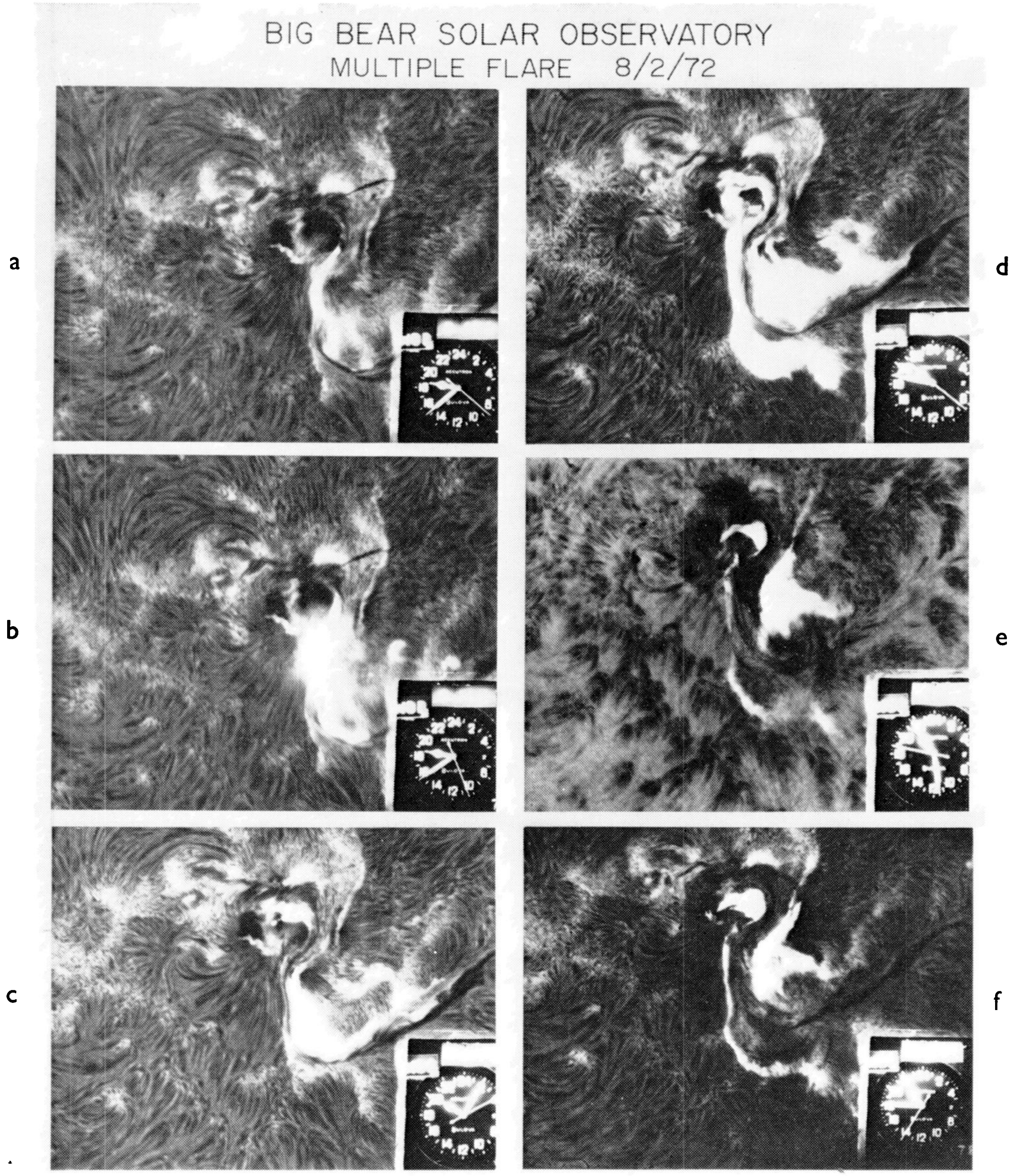

Fig. 11. An Hα centerline sequence of the flares after 18:35 UT. Frame (e) (21:28 UT) shows an Hα +0.5 Å picture which reveals the loops raining down after the flare; frame (f) (21:45 UT) shows the peak of the radio burst; note that the emission has shifted to an entirely different location from the fourth frame (20:47 UT) and both p_1 and f_2–f_3 are covered by emission.

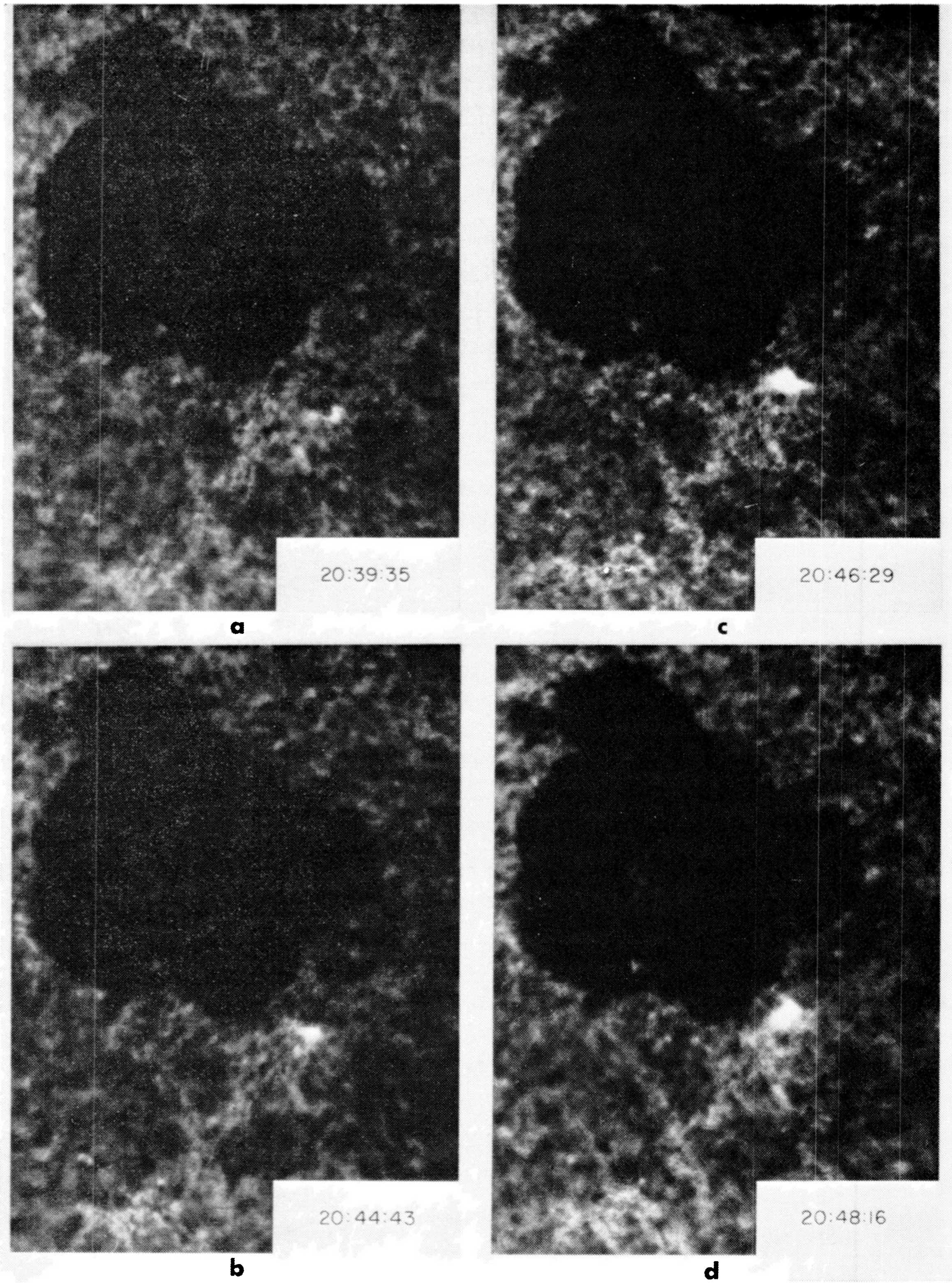

Fig. 12. Dark prints showing the drift of bright points in the $\lambda 3835$ band in the 20:35 UT flare of August 2. The bright points coincide with the Hα bright front (the fourth picture of Figure 11) and move toward spot p_2 with a velocity of 12 km s^{-1}.

radio and X-ray flux. Weak λ3835 emission appeared at this time over the penumbra of f_2. Note that this is different from the decay of other flares, which leave two widely separated strands on the flare perimeter; the emission actually shifted to a different place, and was strong in off-band (Figure 11e), indicating broad Hα profile, and showed λ3835 emission. So there was a real flare resurgence, particularly over the main umbra. The UCSD X-ray data shows a small resurgence of X-ray emission above 10 keV but less than the peak of 20:50 UT. Probably the number of hard electrons was the same, but they occurred in a stronger magnetic field.

The varied aspects of the August 2 flares present an excellent opportunity to compare different flares in the same region. The comparison between the impulsive 18:38 UT flare – small, violent, short-lived – and the large, long-lived, slowly-rising flares at 03:10 UT and 20:00 UT is most instructive. The first can be deduced to be physically low in the atmosphere from the lack of displacement of Hα from the neutral line (despite two days from C.M.P. and the low frequency radio cutoff) and it was by far the most brilliant and concentrated. It also produced a short-lived, intense hard X-ray burst with a spectrum proportional to $\nu^{-3.5}$. The λ3835 observations show the impulsive nature very well. Recent work by Zirin *et al.* (1971) and by Ramaty and Petrosian (1972) shows that a microwave spectrum steeply rising to high frequency indicates a low source height, because the processes, such as plasma cutoff, Razin effect, or free-free absorption that cut off the low frequency synchrotron emission can only take place at lower heights. The sharp cutoff (Figure 14) in the 18:38 UT flare confirms its low height. The 03:10 UT and 20:00 UT flares were by contrast complex and slow, with longer rise times both for Hα and energetic electrons, and radio emission appeared at low frequencies, showing that the events reached high in the atmosphere. Since radio flux and X-rays are proportional to the total number of electrons, we can see how the large volume involved produced the huge radio bursts. However, these large events were less impulsive and had a steeper electron spectrum, so high frequency radio emission was less; for example, at 35 GHz the 21:40 UT peak is only slightly higher than the 18:39 UT peak, although it is 20 times higher at 8.8 GHz. We may conclude that slow events may accelerate particles quite well, but that impulsive, low-lying flares produce the hardest spectra. Finally we have the peculiar (but not rare) effect of the greatest radio burst occurring late in the event without an accompanying large change in the optical flare; apparently once the electrons >100 keV are produced, phenomena over the greatest spots can produce great fluxes of radio emission (because the emission is proportional to the magnetic field strength).

5. The λ3835 Flashes and Impulsive Bursts of X-Rays and Microwaves

The λ3835 flashes in the 18:38 UT flare of August 2 occurred simultaneous with the impulsive hard X-rays and radio bursts. Since good data were obtained in UCSD X-ray experiments and at Sagamore Hill for microwave bursts, it would be useful to compare these three wavelengths for better understanding of electron accelerations in the impulsive phase.

Figure 13 shows comparison of the light curves of several λ3835 flashes with X-rays and radio bursts. Each light curve was made by measuring the brightness of a 3 arc sec^2 area which showed several resolved and/or unresolved flashes in the whole lifetime (1 min) of the flashes with a mean lifetime of an individual flash less than 10 s. (For example, in Figure 10, point (A), the topmost at 18:39:44 UT, is made up of at least 5 points.) One can see that the intensity of the optical flashes peaked around the

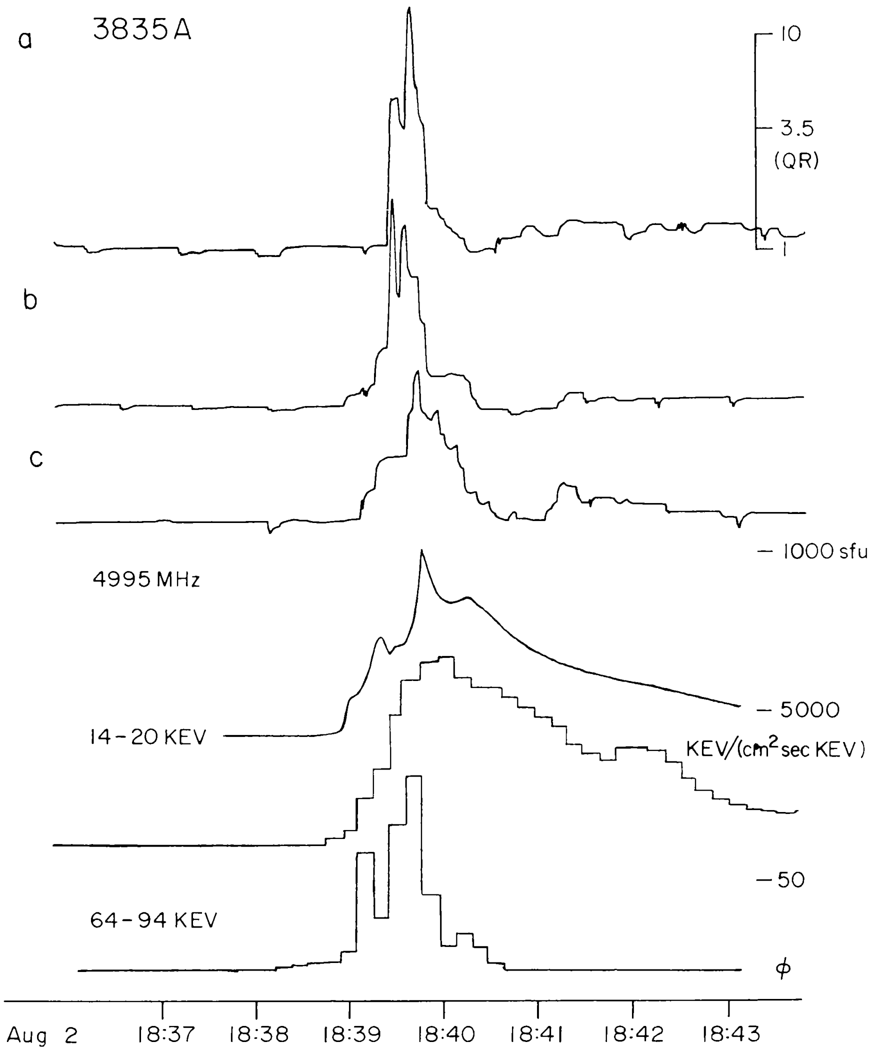

Fig. 13. Light curves of the λ3835 flashes measured at three positions (see Figure 10 for identifications of positions). The lower three curves show a microwave burst (Sagamore Hill) and two channels of hard X-rays (UCSD). Note that the time histories of the λ3835 flashes are most similar to the 64–94 keV burst.

same time as the X-ray and radio bursts and that the light curves are more similar to the X-ray bursts above 50 keV than to the 14–20 keV X-rays or radio bursts at 5000 MHz. In addition, Figure 10 shows that the first flashes appear at 18:39:04 UT simultaneous with the first X-ray spike, and the most flashes were seen at the peak around 18:39:40 UT. The X-ray spectrum was proportional to $\nu^{-3.4}$ at the peak and softening of the spectrum began from 18:40:10 UT (Datlowe, private communication).

The observed intensity of the $\lambda 3835$ flashes can be explained by Balmer line (H9) emission centered at $\lambda 3835$. When we look at spectra taken in another large 2**B** flare, November 18, 1970, observed by K. Tanaka (unpublished) at Okayama, we find wide and large emission of H9, which has 4 equivalent Å of the mean intensity level of $\lambda 3835$ region (20% of the true continuum). We require, in this intense flash, emission of H9 greater by a factor of two than the above flare; if we equate the observed flux at the peak of the flash (equal to the intensity of $\lambda 3835$ in quiet region) to $n_9 A_{92} h\nu L/4\pi$ (L: thickness of the emitting layer; A_{92}: rate of spontaneous emission; n_9: number density of level 9) we get $n_9 L \sim 1.7 \times 10^{14} \text{cm}^{-2}$. Assuming a Saha-Boltzmann distribution with a temperature of 10^4K, we have $n_e n_p L \sim 4.2 \times 10^{33} \text{cm}^{-5}$ at the peak (n_e, n_p are electron and ion number density respectively). The total flux emitted by the flashes may be estimated by adding line emissions, free-bound and free-free continuum emissions radiated from this $n_e n_p L$. With a mean area of the flashes $6 \times 10^{16} \text{cm}^2$ (=10 flashes) we have 2.6×10^{27}erg s^{-1} at the peak. Note that half of this energy flux is radiated in Hα. Actually in dark prints of Hα, we could see Hα brightening simultaneously with the $\lambda 3835$ flashes, but they remained bright after the latter disappeared because of the large opacity of Hα. Precipitation of low energy electrons below 20 keV, which existed till late (as Figure 13 shows), or thermal conduction produced continued heating of the upper layer emitting Hα.

It can be shown from the X-ray flux that electrons above 45 keV in the thin target model and above 60 keV in the thick target model have the same total energy as the optical flux estimated above. 50 keV electrons can penetrate the column density $n_p L \sim 10^{20.4}$ as the theory of Coulomb collision shows (Schatzman, 1965; Shmeleva and Syrovatskii, 1972; Brown, 1972). Also from the observed production rate of 50 keV electrons in the thick foil model ($=1.0 \times 10^{35} \text{s}^{-1}$) it turns out that these electrons penetrating the chromosphere can ionize 7×10^{20} atoms cm^{-2} s^{-1} by making an ion pair every 33 keV (Fermi, 1949; Hudson, 1972). Therefore we can explain reasonably the heating and ionization of the layer responsible for the $\lambda 3835$ flashes ($n_e n_p L \sim$ $\sim 4.2 \times 10^{33}$) by the dumping of the electrons above 50 keV. We have $n_e \sim 10^{13.2} \text{cm}^{-3}$ and $L \sim 10^{7.2}$cm for the emitting layer. Similarity of time profiles between the $\lambda 3835$ flashes and X-ray bursts above 50 keV (Figure 13) would support this explanation. Because of confusion with the other flares we do not know if there was any proton production involved in this fast event, but the fact that γ-rays were not detected gives an upper limit of proton flux less than 3×10^{26}erg s^{-1}, below the energy flux of the optical flashes.

Optical evidence of electron precipitation seen in the $\lambda 3835$ flashes would give a more realistic image of acceleration; impulsive acceleration of electrons occurs in each individual flux loop with a time constant less than 10s and the place of acceleration moves around with the same time scale. Since the flux loops have small cross sections at their ends (0.5″, size of the flashes) and stretch flat on the surface as Hα fibril structure shows, the acceleration must have taken place at a low height ($h < 10^9$cm) and in limited regions. Thick target emission of X-rays (Hudson, 1972) is realistic since most of the electron energy is dumped in a short time at the high density layer.

Even if trapped electrons exist and emit X-rays by thin target, the emission must be small compared to the observed flux, which could be emitted in denser layers by electrons needed to explain the optical flashes.

Radio spectra observed by Castelli (Figure 14) show an increase of flux from 15 GHz to 35 GHz with a dip around 15 GHz. In coincidence with the end of the λ3835 flashes and the X-ray flux in the hardest channels the flux at 35 GHz decreased appreciably showing a single peak spectrum by 18:40:40 UT. If the dip in the otherwise

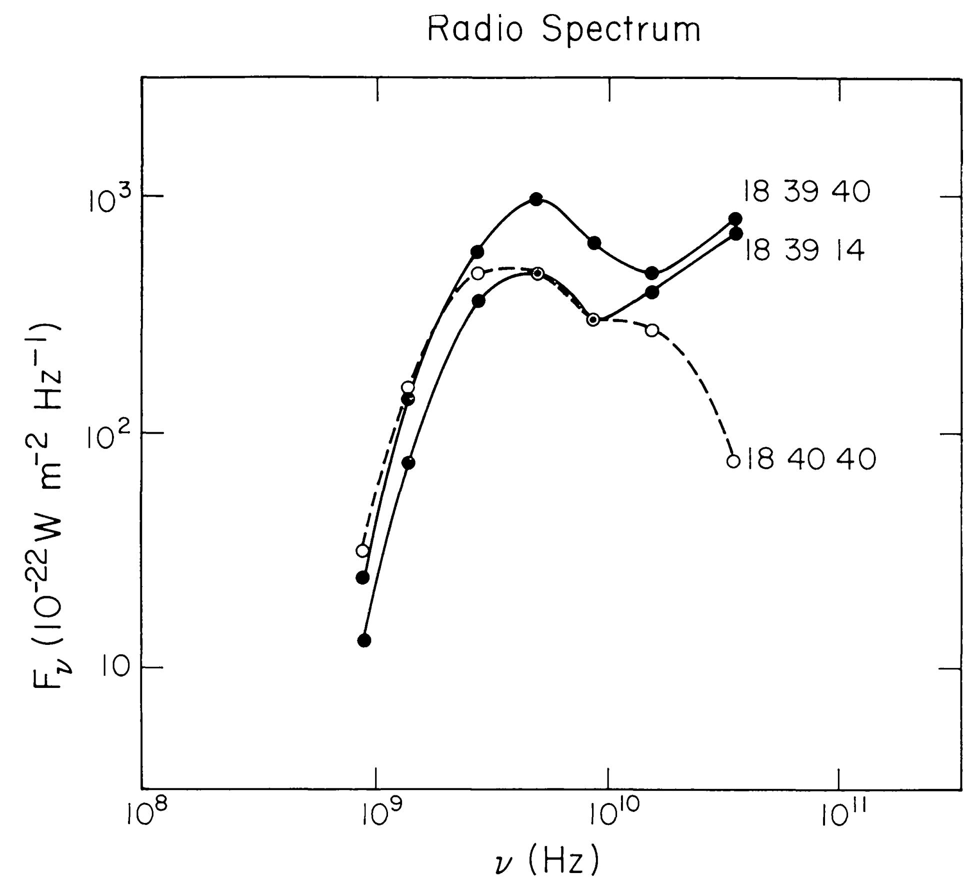

Fig. 14. Microwave spectrum for the 18:38 UT flare of August 2 obtained by Castelli. Note the rapid decrease of the flux at 35 GHz after 18:40 UT, which was in coincidence with the end of the λ3835 flashes.

flat spectrum is not an observational effect, it might be explained by free-free absorption due to hot ambient plasma, which has been proposed by Zirin *et al.* (1971) and by Ramaty and Petrosian (1972) to explain flat type spectrum. In order to realize a dip in the spectrum, it turns out that there must be an optically thick plasma for free-free absorption at the frequency at least 40 GHz. Since hot plasma emitting soft X-rays is transparent for free-free absorption down to 4 GHz as the observed emission measure and temperature show, lower temperature material such as produced the XUV flash must be invoked for the absorption in this model. The double-peaked spectra may also be interpreted as originating from two sources; one at the top of the flux loops, where acceleration takes place with lower magnetic field and plasma density and giving a peak at 5000 MHz, and the other is located at a lower height near the mirror points with a stronger magnetic field and a peak beyond 35 GHz; the flux around 15 GHz may have been depressed due to cut off by plasma frequency or Razin effect or free-free absorption of low-temperature material. These two sources may well correspond to Hα bright points and diffuse halo respectively (Figure 9).

For these two models we may estimate the number of electrons needed to explain the radio fluxes and compare these with X-ray observations. In the case of a homogeneous source model with free-free absorption, we have a total number of electrons above 100 keV (denoted as N_{100}) equal to 10^{34}–10^{35} by fitting the observed spectra to those calculated by Ramaty and Petrosian (1972). This number is not inconsistent with $n_i N_{100} \sim 10^{45.6}\text{cm}^{-3}$ derived from the X-rays by assuming thin target although the thin target model is not realistic for explaining the λ3835 flashes. In the thick target case we have $\mathrm{d}N_{100}/\mathrm{d}t \sim 1.6 \times 10^{33}\text{s}^{-1}$; so accumulation of injected electrons for 10s or more is necessary. This does not agree with the thick target picture. On the other hand, when we consider a flux loop model in which acceleration takes place continupusly for 10s or less at the top, and electrons dump at the two ends of the loop emitting X-rays there by thick target the total number of electrons in the flux loop at any instance can be determined by the continuity equation along the flux loop: $v(N_{100}/L) = (\mathrm{d}N_{100}/\mathrm{d}t)$, where L is a length of flux loop. With $v \sim c/2$ and $L \sim 2 \times 10^9$cm (observed mean distance between pair flashes) as well as $\mathrm{d}N_{100}/\mathrm{d}t$ from the thick target model we have $N_{100} \sim 2.1 \times 10^{32}$, in agreement with $N_{100} \sim 10^{32}$ obtained for the 5000 MHz peak of two source models. To drive the latter number, optically thin gyro-synchrotron emission is assumed with the peak emission occurring at $3v_B$ (Takakura, 1967) since self-absorption would be negligible in a small cross section of a flux loop such as is considered here. ($N_{100} = 10^{32}$ together with $B = 500$ G and $A = 2 \times 10^{18}\text{cm}^2$ gives a self-absorption factor $N/BA \sim 10^{11}$, which agrees approximately with the calculated curve by Ramaty and Petrosian (1972) if we adopt the electron power equal to 4.5 obtained from the thick target in this case.) For the higher frequency peak we get a similar value for a magnetic field larger than 1000 G although we don't know the exact frequency and flux of the peak. Thus we can explain the radio flux in this simple model of a flux loop consistently with thick target X-ray emission and the 3835 flashes. It is to be noted that the electron distribution exponent $\gamma(N(E) \sim E^{-\gamma})$ derived from the high frequency slope of the radio spectrum at 18:40:40 UT (single peak) is equal to $\gamma = 4.7$, in agreement with $\gamma = 4.9$ derived from the hard X-ray spectrum assuming thick target. In the thin target model, on the other hand, we have $\gamma = 3.0$, inconsistent with the radio value.

6. Developments August 3 to 4

After the great events of August 2, the region changed rapidly: the spot p_1 continued to grow and plow into the p region, f_2 and f_3 split apart and a small EFR appeared between f_1 and p_1, eventually producing some new f spots. The axis of f_2–f_3 rotated rapidly as f_3 moved eastward, producing further shear along the neutral line. A series of small flares occurred during August 3, the largest being at 22:10 UT, with arms around p_1 and area between f_2 and p_3, where p_3 was approaching ever closer to f_2.

When the Sun rose at Tel Aviv on August 4, a great flare was beginning; observations began at 06:24 UT showing the flare rising to a peak area at 06:35 UT. But the most rapid rise occurred between 06:24 UT and 06:27 UT, coinciding with the steep rise and peak in the radio burst. The Hα flux 1.0×10^{27}erg s^{-1} (using August 7 line widths) was constant from 06:25 UT to 06:45 UT and decayed slowly. As on August 2, 21:45 UT, the greatest peak in the radio emission came with brilliant emission covering the *f*-spot. Figure 15 shows the peak of the flare photographed at Tel Aviv.

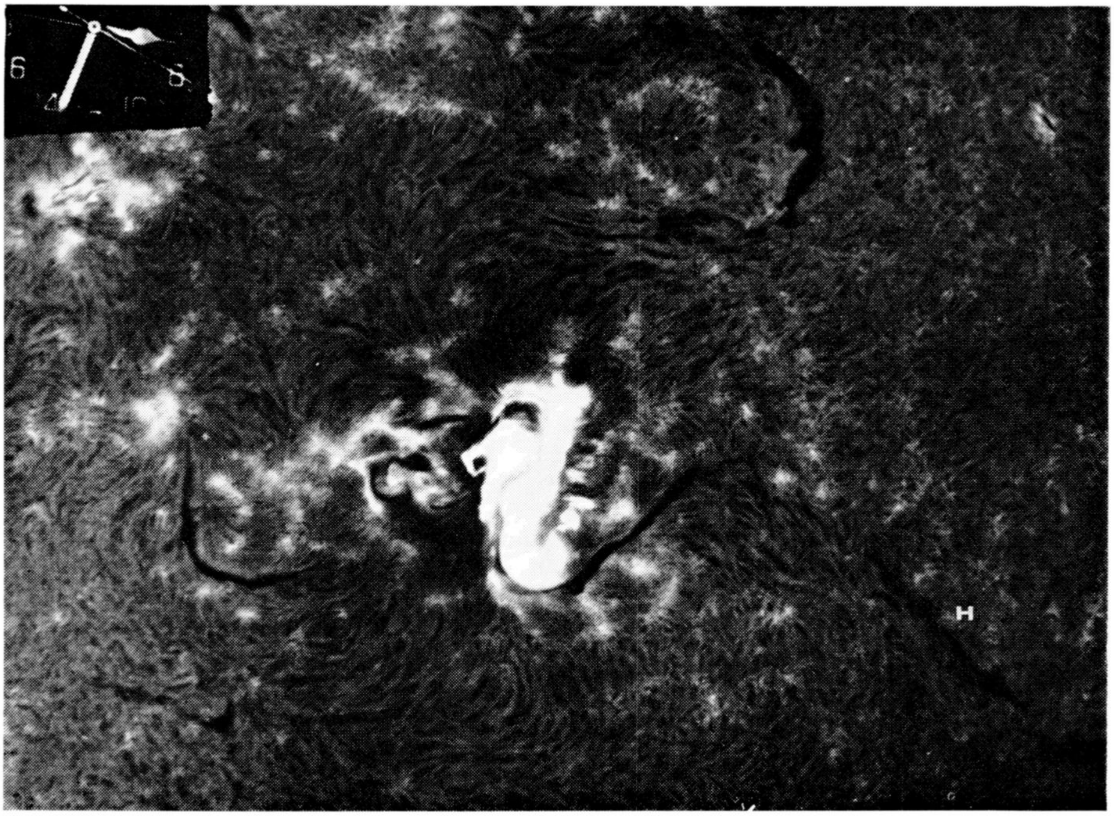

Fig. 15. Maximum of the August 4 flare, 06:34:19 UT, photographed at Tel Aviv. This is a classic two strand flare, leaving two faint thin rims at the extreme edges for many hours. The filament H was disturbed by the flare.

It was a classic 2-strand flare, with most of the area in the *p*-polarity, and it did not have the irregular growth of the August 2 and 7 flares, nor was it so impulsive as the much smaller event of 18:38 UT August 2, although a rise in radio flux of 26000 sfu in 3 min is certainly not sluggish. Thus its radio spectrum fell off somewhat above 8.8 GHz. The radio flux reported by Slough dropped off after the flare passed maximum. At 06:42UT a group of bright loops passed across from the f to p side, filling the space between the two strands; these became dark 10 min later. Again, although the field lines on the surface run tightly parallel to the neutral line, the loops high above are perpendicular. We see the loops increase their tilts to the neutral line continuously with time (see curve in Figure 19 for this change). The bright strands faded and separated, leaving two thin strands at the farthest points from the neutral line, lasting many hours. This, and the slow decline of thermal X-ray emission (*e*-folding time equal to 150 min), shows how the coronal cloud produced by the flare cools from the surface outward, leaving only the outermost loops at the end. These loops presumably produce the Hα strands by thermal conduction at later phases.

No Moreton wave appears on the film; although the observations are in Hα centerline, a Moreton wave should be visible. However, a section 0.6 $R_\odot$ from the spot of the long filament stretching E of the spot (*fil 1*) disappeared at 06:26 UT; and an emerging flux region 0.7 $R_\odot$ from the flare brightened about the same time. These distances imply a wave moving 1000 km s^{-1} from a source at 06:18UT (the earliest reasonable time, judging by radio data), but moving above the chromosphere so that it is seen only indirectly. More interesting, a bright wave or spray moved out from a point in the filament about 0.6 $R_\odot$ from the flare at 06:24 UT with a velocity of 250 km s^{-1}. This wave, which moves irregularly N-S from the filament, looks like a slow Moreton wave. If it was triggered by an invisible wave from the flare, we again get 1000 km s^{-1} for the velocity. We have not seen such a phenomenon before. The filament waves about continually until 08:00 UT.

Uchida (1972) has shown that the Moreton wave may be considered as an MHD wave which only touches the surface when it reaches a region where the Alfvén velocity is low and a steep shock develops. It may be that the wave in question did not touch the surface,but was able to affect the chromospheric features it passed by perturbing the field structures. The apparent triggering of a slower wave from the prominence is obviously a more complicated problem, either involving energy stored in the prominence or refocusing of the wave energy.

7. Development August 4 to 7

In the BBSO pictures for August 4, we can recognize several changes which may be connected with the August 4 flare. p_1 and p_2 had grown, and the spot p_3 moved in ahead of f_2, almost touching it. A tight filament twisted in between them, and the field gradient was very large indeed. Although p_3 did not take obvious part in the flares, its motion to west was every bit as remarkable as that of f_1 – in fact on August 6 the filament passes around p_3 and it is an island of *f* polarity inside the *p* penumbra. Although the group gave the appearance of an extremely active one, there was in fact little activity aside from the great flares. Most of the smaller flares were two-strand or two-point flares which may be used to determine the ends of flux loops, for example one at 01:02UT August 5 connected f_1 and p_3 and several flares connecting f_3 and p_1.

Probably the most important consequence of the August 4 flare was the rapid separation of f_3 from f_2. As can be seen in the off-band pictures of Figure 4, f_3 appeared separate from f_2 at dawn on the 3rd and steadily drew apart, producing a winding in the neutral line between p_1 and f_3. There was also a rapid motion of p_2

towards p_1 after August 4. This motion occurred in the opposite direction to the movement of f_3. It is likely that both motions worked to increase the shear of the filament between them. These spot motions were generally very slow with a mean velocity 30 m s^{-1}–50 m s^{-1}. But they occurred steadily and in two or three days there were always noticeable changes in spot configurations as well as large increases of shear in the neutral line. Obviously such changes were necessary for a big flare to occur as the observed intervals between big flares show.

There were no more flares with footpoints in f_2. There was considerable small surge activity in the area just following f_3 on the E side of the neutral line. Such activity is characteristic of emerging flux, and the magnetograms for August 4, 5, and 6, in fact, show f polarity which was part of the emerging dipole imbedded in the p polarity region (Figure 7). Dark fibrils connected this flux to p_1. Eventually on August 7, the *f* flux broke through and filled this region. Small flares at 01:37 UT and 16:53 UT on August 5 extended along the dark fibrils from the EFR to p_1 and f_3, while the flare at 01:00 UT had just two bright points at f_1 and p_3. There was also rapid growth of new *f* spots following f_1 and just across the neutral line from p_1.

On the 6th, the dark filament, *fil 1*, now stretched all the way through the region and around to the W side. It was, of course, no ordinary filament, but a complex of twisted dark fibrils along the neutral line. Spot f_3 shrank and there were penumbral fibrils parallel to the neutral line (east-west). Large velocity shear was observed in this penumbra on August 7. During the 6th, dark loops were visible on the red wing of Hα, pouring down into p_1.

8. The Great Flare of August 7

Observations at Tel Aviv showed high plage brightness in the early hours of the 7th; when observations began at Big Bear at 13:50 UT, there was a flare in progress following p_1. OSO 7 shows a steady increase in soft X-rays beginning at 10:00 UT. The filament winding E of f_3 was continually active, and a small flare encircled f_3 at 14:42 UT. Hα spectrum scans taken at 14:50 UT showed very wide and slightly tilted absorption features at A (Figure 16) with a Doppler width of 80 km s^{-1}, indicating filament activation. A wavelength scan at 15:00 UT shows strong λ shifts. The cancellation picture (Figure 16) between $+0.5$ Å and -0.5 Å shows that the activated filament started rising at point A (bright in the figure), and that the other parts of the filament were mostly falling. Note that narrow rising threads were seen in contact with the falling filaments indicating a rolling motion of the filament. At 15:03 UT the dark feature in the blue wing was moving along the filament from A to B. This was followed immediately by the beginning of the flare at 15:05 UT. The BBSO observations are simultaneously at ± 0.5 Å with 7 s intervals between frames. The first bright points appeared simultaneously over the p_1 umbra, directly across the neutral line in the new spots following f_1, along *fil 1* N of p_1, and just preceding f_3. At 15:12 UT a bright streak flowed N (down) from spot p_1 along *fil 1* into the northernmost bright element; at the same time the bright f-points connected. This phase is seen in the first frame of

Fig. 16. Picture showing the cancellation between +0.5 Å and −0.5 Å of Hα at 15:00 UT on August 7. Bright is rising, dark is falling for the filaments. The position of the spots is shown by broken lines. At the rising part (A) of the filament, the absorption spectrum with 1.8 Å wide (Doppler width) was observed at 14:52 UT. *Note added in proof:* for P_3 read F_3 (F_3 should be ignored).

Figure 17. Now the main growth took place in the f-region, first (15:15 UT) preceding f_3, then (15:18 UT) on the arc from f_1 to f_3. This brightening flowed along to f_2 then bounced back at 15:21:00 UT, and when it hit the neutral line at 14:22 UT there was an enormous brightening all over, particularly in the *f*-polarity, including, for the first time, the *p* polarity area directly across from f_3. This was the peak of the flash phase and appears to agree with the peak of the radio burst. However, spectra and dark prints show that the newly brightened area was much fainter than the two flare kernels. The flare continued to grow, albeit more slowly, particularly spreading over all the *f*-spots except f_1 and forming an elegant sea-horse shape. On the 37 GHz records from Slough there are peaks at 15:16 UT, 15:18 UT and 15:21:5 UT, which appear to correspond to the stages enumerated above; this confirms our feeling that 'quasi-periodic' microwave and X-ray pulsations, noted by Frost (1969) are just successive energy releases in different areas, the time spacing being the time it takes an MHD wave to cross the region. Where such velocities are seen as the advance of distinct bright fronts, we measure about 600 km s^{-1}. However, if we look at the flare on a dark print (Figure 18), we find that only two areas over p_1 and the curved branch on the *W* side are very bright – the rest of the Hα flare is much weaker and only ap-

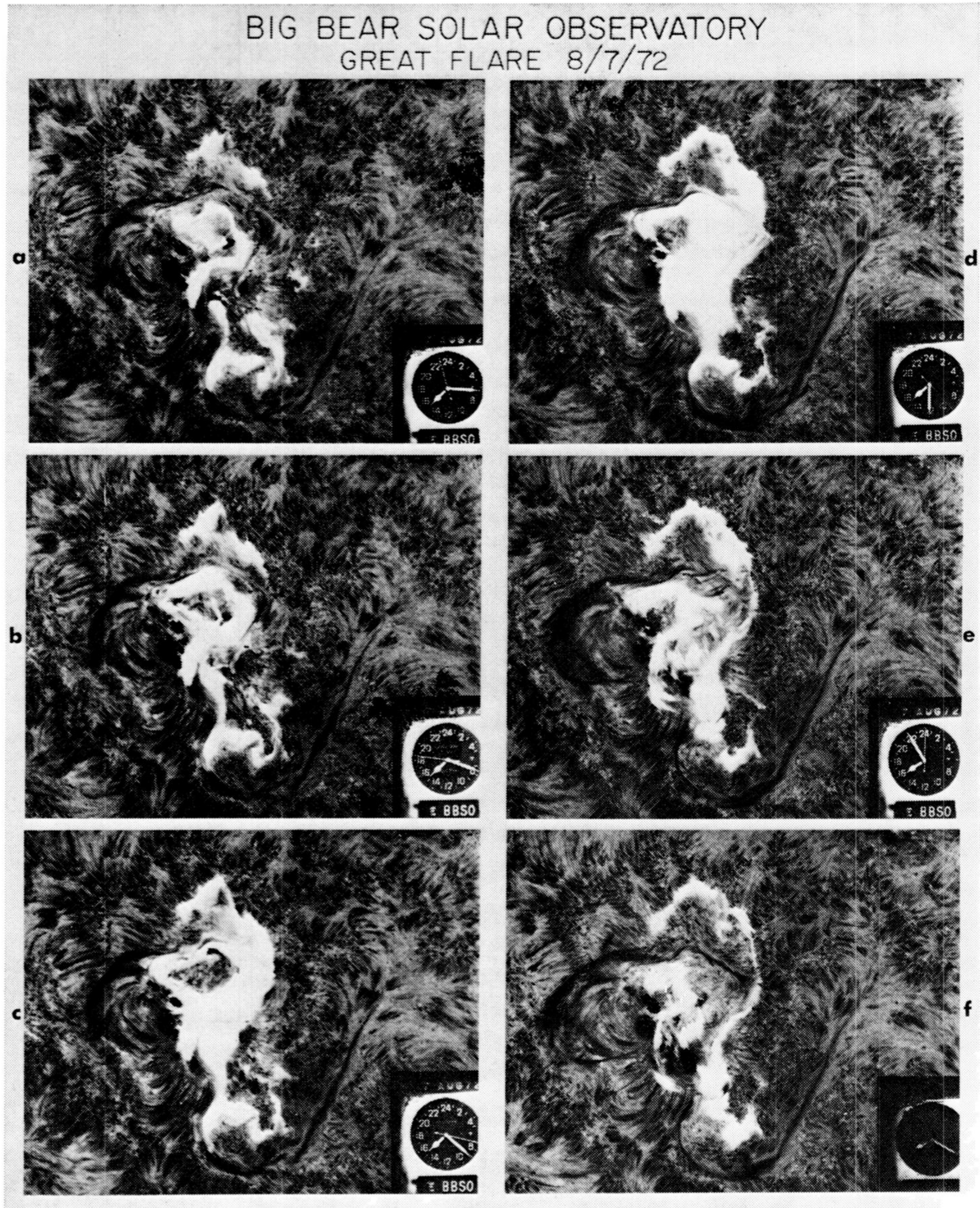

Fig. 17. Development of the August 7 flare, Hα $-\frac{1}{2}$ Å. The intense kernels are located in p_1 and the lower half of the area curling just above the neutral line. Note the bright strands in the late phase of the flare.

pears as bright because of the saturation of the print. Note that *fil 1* was completely disrupted in the flare region but relatively unaffected outside. At 15:28 UT the first bright loops (obviously corresponding to the loop prominences one might see at the limb) appeared crossing in the center of the flare, almost parallel to the neutral line (Figure 18). With the disappearance of these loops, new loops (dark in later phases)

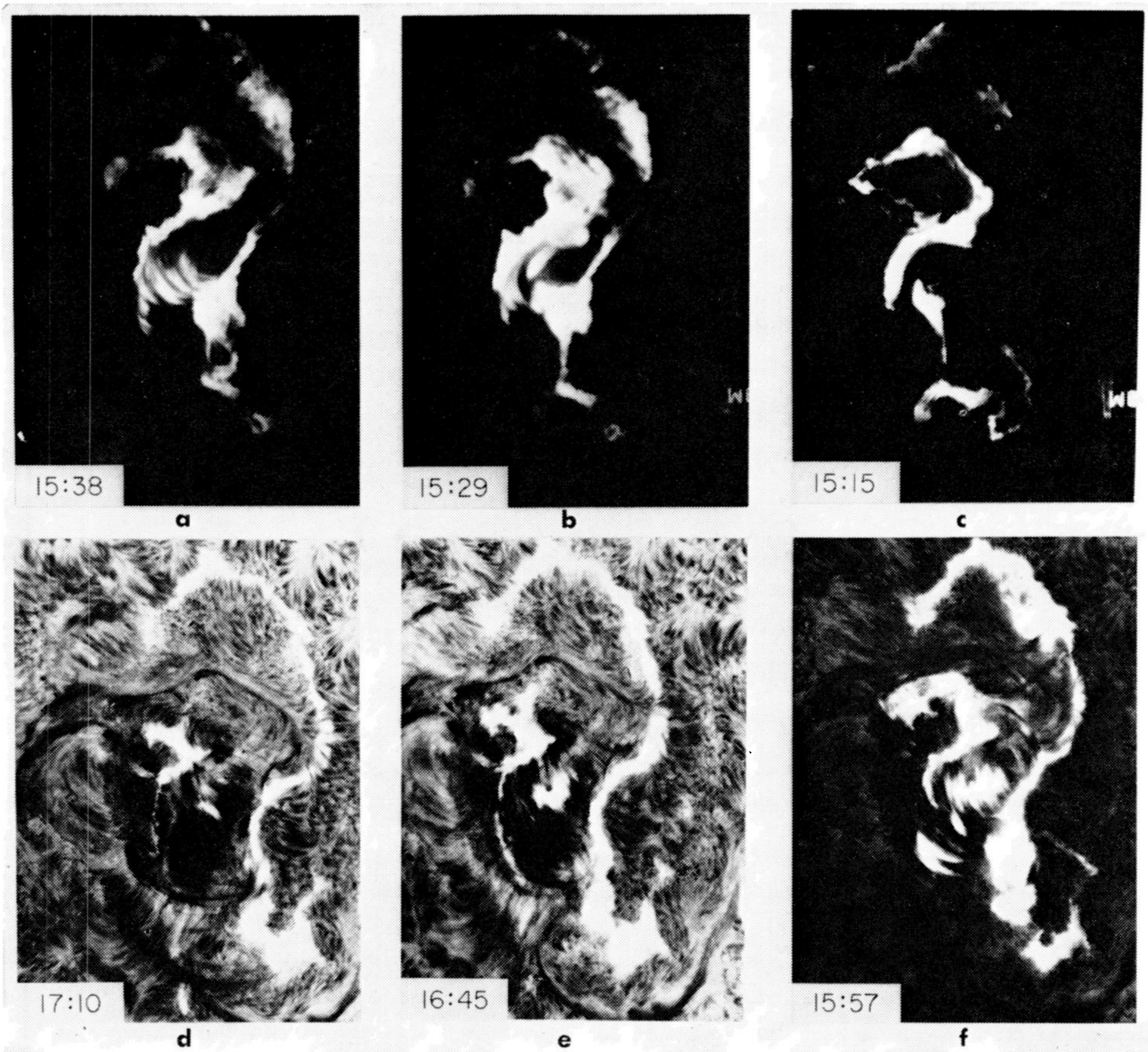

Fig. 18. Dark prints showing the development of the flare loops in the August 7 flare, $H\alpha + \frac{1}{2}$ Å. The first loop appeared at 15:29 UT, crossing the neutral line at a sharp angle. The loops are dark in (e) and (f) except the center.

successively appeared, making greater angles to the neutral line. Figure 19 shows time variation of the tilt of the loops to the neutral line at various places in the center of the flare; it increased rapidly until 15:40 UT, and continued to increase slowly in the late phase of the flare. Similar changes in the loops were also observed in the August 4 flare showing the same time history as this flare (indicated by a line in Figure 19). Loops were connected at foot points to the two emission ribbons, which moved steadily outward with a velocity of 2 km s^{-1}.

Apparently the loops formed later higher than those formed earlier. We could actually see in later phases of the limb flare of August 11 that semi-circular loops appeared successively at higher places with the apparent rising velocity of 1.7 km s^{-1}, which was about equal to the separation velocity of the two ribbons of the August 7 flare. We may conclude from this change of tilts that the field at the surface runs along

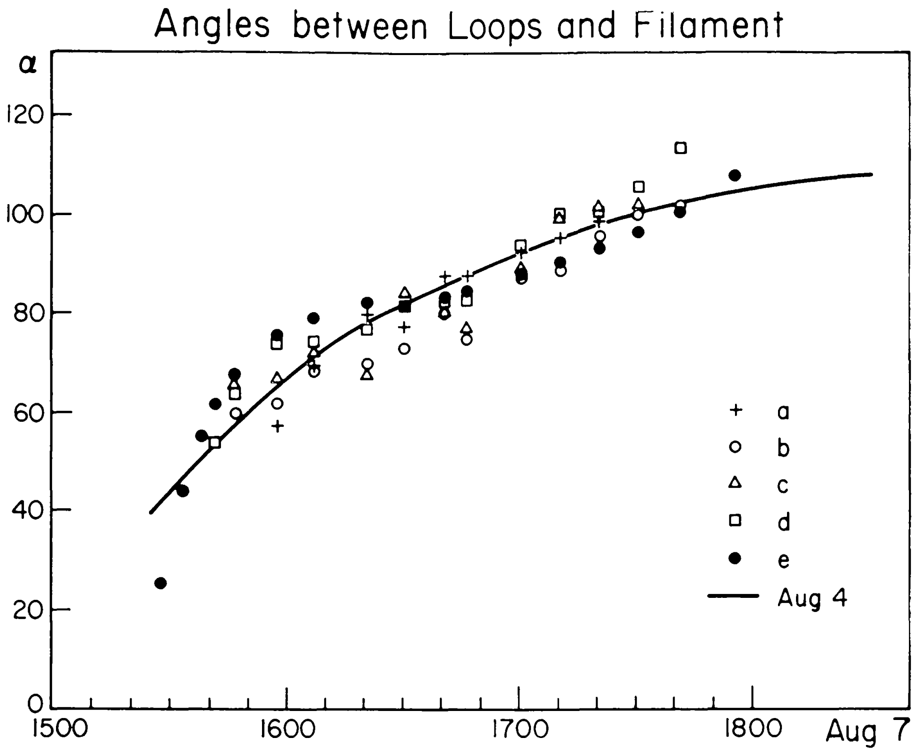

Fig. 19. Time variations of the angles between the loops and the filament (the neutral line) at the center portion of the August 7 flare. The line shows the similar variation in the August 4 flare. (The time is shifted to match the August 7 case.)

the neutral line, while at greater heights the field lines run at successively greater angles to the neutral line, getting closer to a potential field which connects p and f polarity with the minimum energy. This sheared structure of fields may have existed from the start; as the flare plasma cools, condensation takes place in successively higher loops. Alternatively, higher loops with less energy may represent re-establishment of potential type field lines after reconnection of low loops, the difference in energy between them being released by some unknown mechanism. This case corresponds to the continuous energy release in the late phase although the release rate slows down much. In any event, we can say that much of the flare energy is due to successive stripping away of long, highly sheared low field lines, and their replacement by potential fields.

Two emission ribbons moving apart were visible for a long time in all the large flares. In later phases on August 7 we could see dark mottles or spicules appeared crossing above the emission ribbons. (See Figure 17f and Figure 18d.) Hα emission in these ribbons must originate low in the chromosphere. We have a flare model in which the hot thermal plasma produced by the flare continuously diffuses outward. This plasma radiates much more energy than normal coronal heating can support, so it cools once the flare energy input ceases. The inner part cools faster, because of its greater density and the short distance to the surface, and the hottest plasma is located at the outer edge. In this model loops appear after the gas has cooled to a temperature at which Hα may be emitted. This implies that the outer shell is denser than the inner after it cools; observations of continuum in the limb loops have showed a peak density at the height of the loop tops.

9. Spectra of the August 7 Flare

James Dominy was observing with the Coudé spectrograph, and spectra were taken beginning at 15:00 UT at 10 s intervals in Hα. Although the flare spectra are only in Hα, they are particularly valuable because we have simultaneous slit jaw and filter observations, because the spatial resolution is good, and because the spectra were taken throughout the flash phase. Until 15:16 UT, spectra were taken of the bright area N (below) p_1; at 15:16 UT the spectrograph slit was shifted to the main bright f kernel and its development followed. The spectra are shown in Figure 20 and the time dependence of total Hα flux from planimetered microdensitometer tracings is in Figure 21. There were two intense kernels of emission in the f area, which showed maximum line width 12 Å (FWHM) for a few minutes around 15:20 UT (Figure 20). Peak intensities up to three times the local continuum level were observed. Profiles at this stage showed red asymmetry due to additional emission of 3 to 10% in equivalent width, centered on 2 Å red, but the peak emission still was at line center. This shift corresponds to the velocity imparted to protons by collisions with electrons moving near the speed of light and may be due to atoms excited or accelerated by collisions with downward moving fast electrons. There is a basic asymmetry in the geometry; if electrons are accelerated above the surface, as one can suppose, then they can only collide with much material when they move downward, hence a red asymmetry would result. It is to be noted that no red asymmetry appeared (in these kernels) after 15:21 UT, when the flux of radio emission ($\nu \leqslant 8800$ MHz) was still rising. This radio emission reached maximum about 15:39 UT. Hα fluxes of kernels started to decrease from 15:25 UT, but the area of emission was still increasing, showing peaks at 15:28 UT. Thus the total flux of Hα emission stayed rather constant from 15:20UT to 15:28 UT.

When emission spread rapidly from f_2 to all the p and f area at 15:22 UT (corresponding to the last peak of the 37 GHz emission), weaker red shifted emission was observed at the outer part (p) of the filament (Figure 20, 15:23 UT). Filtergrams at ±0.5 Å showed much more intense emissions in the red wing than in the blue wing over the whole p area and part of the f area. The emission profiles measured could not be classified as the asymmetrical ones which have been reported before (see review by Švestka, 1972; Smith, 1973), but show a peak at 2 Å red from line center. The excess emission can be represented by a Gaussian profile with an equivalent Doppler width of 2.9 Å. This lasted for 5 min and faded after 15:27 UT. This red shift cannot be due to the projection effect of horizontal motion, for the direction of the spread of emission is largely toward us. Thus it must be due to downward moving atoms or downward moving exciters. The total energy of the red shifted emission is estimated as equal to 6×10^{28}erg, which is only a small fraction of the energy of non-thermal electrons. After the rapid spread of the flare the red-shifted emission was replaced by relatively narrow emission symmetric about the line center.

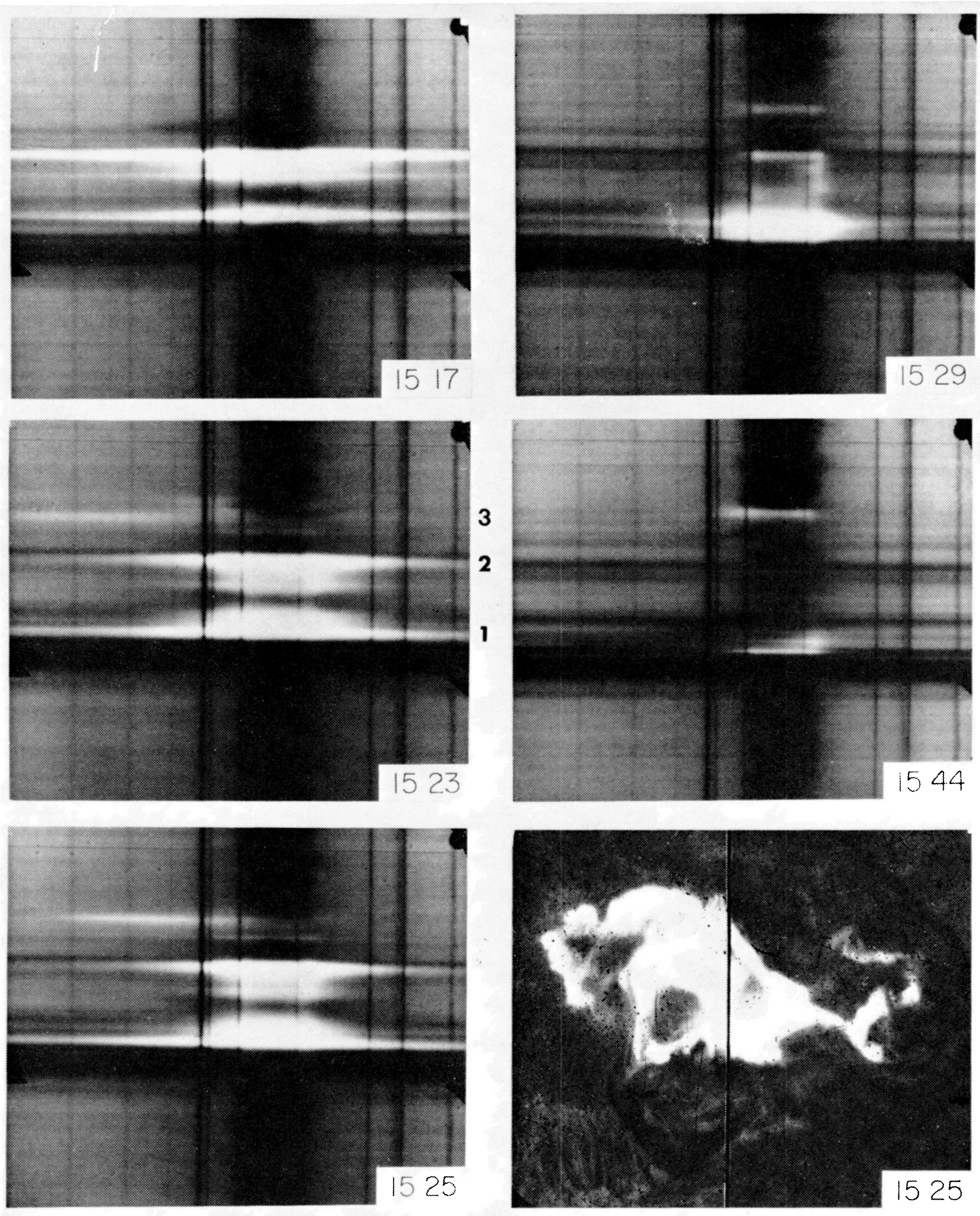

Fig. 20. Sequence of Hα spectra taken at the flash phase and the later phase of the August 7 flare. The spectrum covers 10 Å. Dispersion 0.56 Å mm^{-1}. Red is to the left. The slit jaw Hα picture at the lower right shows the slit orientation. Note the strongly red-shifted emission (3) at 15:23 UT and 15:25 UT. Only the kernels (1) and (2) are really broad.

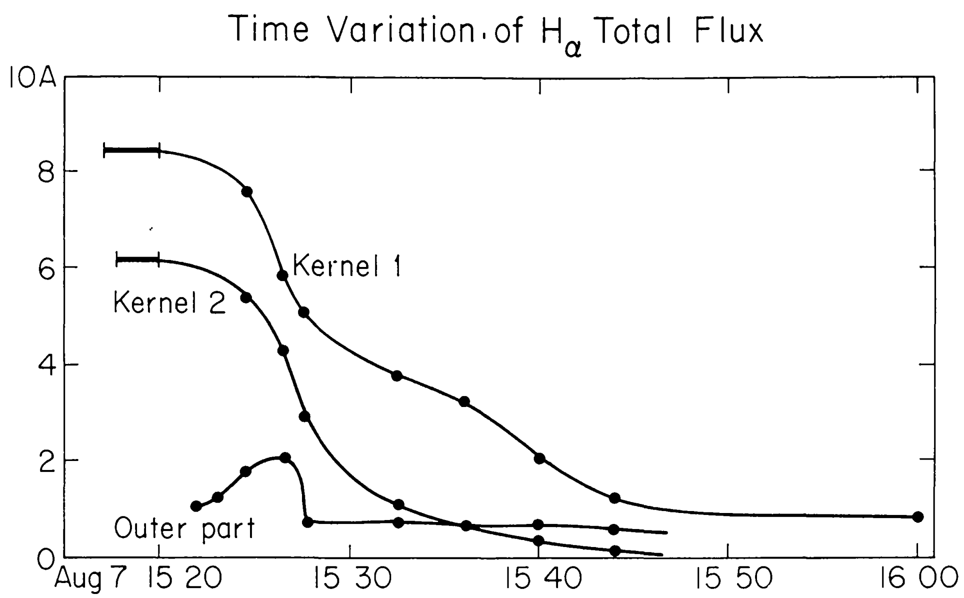

Fig. 21. Time variation of Hα total fluxes denoting the net energy between the emission profile and the absorption profile at the quiet time. The energy is shown in wavelength units, referring to the continuum of the quiet region. See Figure 20 for three measured places. (The 'outer part' is point (3).) Note that maximum for the flare area was attained at 15:28 UT after the widest emission disappeared.

We must emphasize that all the emission, shifted or unshifted, occurring outside the kernels was relatively narrow and weak compared to the great emission from the flare kernel itself. We can conclude that the main energetic flare occurs in the kernels, and the outer areas are 'lit up' as the flare energy spreads to higher flux loops and hot red-shifted material rains down on the surface. The small red asymmetry in the kernel may be due to superposition of the downward falling bright material which covers the flare area of precipitating particles.

The Hα width dropped below 1 Å after 15:45 UT even in the strongest kernel.

Late in the flare, spectra were obtained in various spectral regions, scanning over the whole flare area. They show a remarkable velocity discontinuity in the photosphere between p_1, p_2 and f_3 in a region which shows penumbra but no sunspot (Figure 22, x on the slit). The shear is seen in the spectrum to occur in all spectrum lines, it amounts to 4 to 5 km s^{-1} to the red side, irrespective of line strength, or over 6 km s^{-1} if the motion is in the surface plane of the Sun. The motion was seen in spectra up to 19:00 UT, whereupon it stopped. The photospheric motion associated with a flare has been reported by Yoshimura *et al.* (1971) although there is no velocity shear in the motion they found.

Off-band pictures before and after the flare show a large change in the direction of the penumbral filaments in this area (just above the x on the slit in Figure 22); at 15:00 UT these filaments were directed to the northwest or to the direction of the slit in Figure 22, while at 20:50 UT their direction changed to the southwest (a direction shown by an arrow in Figure 22), producing a kink between these penumbral filaments and those in p_1. This change may be explained by the sheared flow in the surface

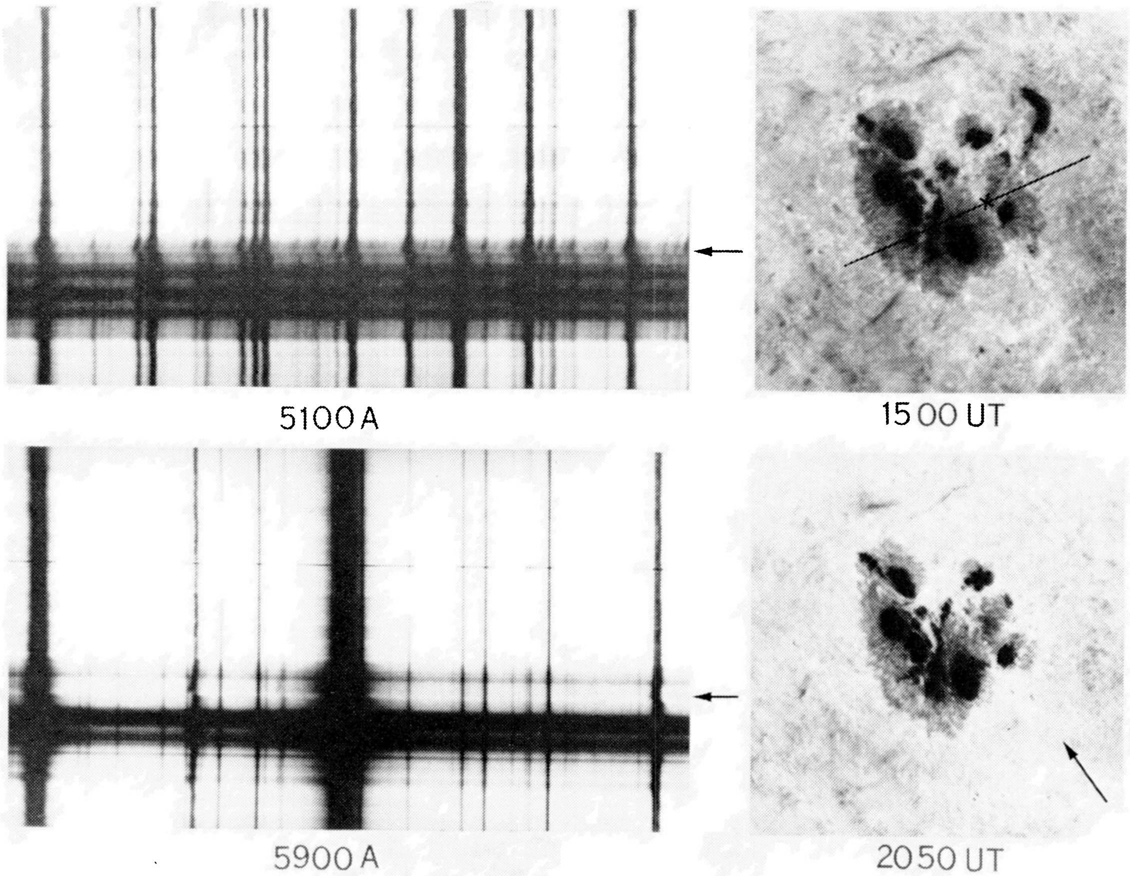

Fig. 22. The velocity shear observed during the flare of August 7 (arrow) in spectra taken at 5100 Å and 5900 Å. The off-band picture at 15:00 UT shows the slit orientation and the place of the velocity shear (point x). The velocity shift is to the red (4–5 km s^{-1}) and appears for all the lines. Note that the direction of the penumbral filaments at point x changed after the flare (20:50 UT) as if the flow occurred along the boundary of the penumbra (f_3) towards the arrow shown in the lower right.

plane seen in the spectra, which dragged the penumbral filaments to the southwest direction. We only measure radial velocity, so the direction of motion may only be deduced from observed changes in penumbral fibrils and the neutral line. The direction of this motion (perpendicular to the neutral line) is such as to increase the shear of the magnetic field lines, as though the photospheric flow is inexorably pushing on either side of it, finally to be released by the flare. Note that this flow was perpendicular to the motion of spot p_2 towards p_1 which was along the neutral line. The activation of the filament before the flare is shown in Figure 16 to occur at the south-east edge (A), along a segment anchored in the moving penumbra (also see dark feature at 15:00 UT in Figure 22).

Study of before-after pairs shows some change in the spot group after the flare. The east penumbras of p_1 and p_2 shrank appreciably, and f_2 and f_3 umbras shrank rapidly. A few small spots under the f kernel changed, but such spots are always changing. There was continued motion of spot p_2 toward p_1, which it joined on the 10th. The largest motion 0.42 km s^{-1} was found during the flare from 15:00 UT to

18:00 UT) The magnetograms show a decrease in the p polarity in the area it vacates, and a general southeast expansion of the p polarity around f_3. The large filament S-W of the p spots, which was active all day on the 7th on the blue wing, disappeared. Further evolution of the group to its limb passage is shown in Figure 6. It gradually simplified and was uninteresting except for the limb flare of the 11th.

10. Hα Flux

There has been much attention paid to the total Hα flux from great flares in comparison with the total energy. In this case, with continuous Hα spectra and filtergrams on both wings of Hα, we can measure this in a more definitive way. We planimetered dark prints (Figure 18) showing two intense kernels at 15:20, 15:27 and 16:00 UT (the end of Hα spectra). At 15:20 UT, the area of the kernels was 6.0×10^{18}cm^2 with band width 9.2 eq. Å (equivalent ängstroms referred to the continuum). At 15:27 UT the area of the kernels had increased to 8.5×10^{18}cm^2 with 6.2 eq. Å width, and at 16:00 UT it decreased to 1.4×10^{18}cm^2 with 1.8 eq. Å width. Time histories of the integrated Hα fluxes are shown in Figure 21 for three places. The total flare area in Hα centerline was 4.3×10^{19}cm^2, but the line width over most of the area was only about 1 eq. Å in the regions outside the kernel. The contribution from these fainter regions to the total energy was 18%, 28% and 87% at three times mentioned. Applying a filling factor 0.74 for the fraction of the kernel that gives the broad emission on the spectrograms (see Figure 20) and correcting for projection, we find a total Hα emission of 1.2×10^{27}erg s^{-1} at the peak. Integrating over the flare lifetime from 15:10 UT to 16:10 UT, with an allowance for the later tail-off, we find a total Hα energy in this huge flare of 2.5×10^{30}erg. We believe that this value would be accurate within a factor 2. We have no spectra for the August 4 event, but we planimetered it and, assuming the same spectrum as August 7, obtained 2×10^{30}erg, roughly the same as August 7.

If we compare this value with the total proton energy estimated by Ramaty and Lingenfelter (1973) as 10^{35} protons above 10 MeV or about 2×10^{30}erg, we see that the Hα energy is comparable to the protons and the hard electrons.

If we consider that energetic phenomena are limited to the kernel from which most of the emission takes place, we may estimate the volume involved by considering it as a loop connecting the two branches of the kernel. Each branch has an area about 1.7×10^{18}cm^2 and the separation is 25000 km, hence for a semicircular loop we get 2×10^{27}cm^3. If the emission measure was $10^{48.3}$ for X-rays above 10 keV (same as August 4 flare), we get $N_e N_i$ equal 10^{21}. It appears that a sizeable fraction of the electrons in the kernel are accelerated.

Finally, the dominance of Hα emission from the flare kernel may explain the discrepancy found between the reported time of 'Hα maximum' (15:30 UT for the August 7 flare) (*Solar Geophysical Data*) and X-ray and radio bursts. A plot of the total Hα energy from the August 7 flare peaked around 15:22 UT, the time of the peaks of radio ($\nu \geqslant 11000$ MHz) and X-ray emission, and remained constant up to 15:28 UT. The same time would be derived from peak kernel brightness and peak Hα line width.

11. Conclusions

(1) The region exhibited inverted magnetic polarity and high gradients from its birth.

(2) The intensity of the flares in this region appears to be due to high field gradients across the neutral line and substantial shear along it.

(3) The motions and growths of sunspots occurred steadily from July 30 to August 7, producing the invasion of p spot into f area and increased the shear of the neutral line.

(4) Development of the post-flare loops revealed sheared structure magnetic field lines above the neutral line; the lowest field runs parallel to the neutral line and the higher field runs more and more perpendicular to it. We believe the flares occur in the transition from the sheared field to the potential field.

(5) The Hα flux of the large flares comes mainly from kernels whose emission peaks with radio and X-rays. The total Hα emission from the great flares of August 4 and August 7 was 2.0×10^{30} and 2.5×10^{30}erg, respectively.

(6) The Hα emission was 12 Å wide (FWHM) in the flare kernels and only 1 to 2 Å wide in the rest of the flare. This flare halo made up most of the area and thus determined the assigned 'importance' but only produced $\frac{1}{4}$ of the Hα emission.

(7) In λ3835 band we detected rapidly varying emission at the ends of the flux loops. The emission can be explained by the dumping of the 50 keV electrons accelerated in individual flux loops.

(8) Comparison of the λ3835 flashes with the X-rays and microwave emissions shows that thick target models of X-ray emission are more consistent than the thin target model for the impulsive flare.

(9) We observed a large velocity shear of absorption lines in the flare region. This explains the rapid change of the fibril orientation observed in the penumbra which may be related to the cause of the flare.

Acknowledgements

We are indebted to many colleagues who supplied their data for this study, in particular to Dr Dayton Datlowe, UCSD, and Dr John Castelli, AFCRL, and James Mosher. We thank also Dr H. Hudson and Dr S. Enome for discussions. The Big Bear observations were made by James Mosher, Tom Pope, David Glackin, James Dominy, David Brin, John Morgan, Douglas Rabin and the authors. A 16 mm film of the flares is available at cost ($30.00). We are particularly grateful to Mr Dale Vrabec for pointing out that our original polarity choice was reversed.

We have incorporated a number of constructive suggestions by the referee of *Solar Physics*.

This work has been supported by NASA under NGR 05 002 034, NSF Atmospheric Sciences program under GA 24015, and AFCRL under FI9628-73-C-0085.

References

Brown, J.: 1972, *Solar Phys.* **26**, 441.
Bumba, V. and Howard, R.: 1965, *Astrophys. J.* **141**, 1492.
Chapman, G.: 1970, *Solar Phys.* **14**, 78.
Fermi, E.: 1949, *Nuclear Physics P.*, The University of Chicago Press.
Frost, K. J.: 1969, *Astrophys. J.* **158**, L159.
Hudson, H. S.: 1972, *Solar Phys.* **24**, 414.
Lazareff, B. and Zirin, H.: 1973, submitted to *Solar Phys.*
Lincoln, J. V. and Leighton, H.: 1972, *Report UAG-21*, World Data Center A, p. 80.
Prata, S.: 1971, *Solar Phys.* **20**, 310.
Ramaty, R. and Lingenfelter, R. E.: 1973, in R. Ramaty and R. G. Stone (eds.), *High Energy Phenomena on the Sun*, NASA Symp., p. 301.
Ramaty, R. and Petrosian, V.: 1972, *Astrophys. J.* **178**, 241.
Schatzman, E.: 1965, in C. de Jager (ed.), *The Solar Spectrum*, D. Reidel Publishing Company, Dordrecht-Holland, p. 313.
Smith, E. v. P.: 1973, private communication.
Smithson, R. and Leighton, R.: 1971, in R. Howard (ed.), 'Solar Magnetic Fields', *IAU Symp.* **43**, 76.
Švestka, Z.: 1972, *Ann. Rev. Astron. Astrophys.* **10**, 21.
Syrovatskii, S. I. and Shmeleva, O. P.: 1972, *S.A.F.* **16**, 273.
Takakura, T.: 1967, *Solar Phys.* **1**, 304.
Tanaka, K. and Zirin, H.: 1973, in R. Ramaty and R. G. Stone (eds.), *High Energy Phenomena on the Sun*, NASA Symp., p. 26.
Uchida, Y.: 1972, pre-print.
Yoshimura, H., Tanaka, K., Shimizu, M., and Hiei, E.: 1971, *Publ. Astron. Soc. Japan* **23**, 443.
Zirin, H.: 1972, *Solar Phys.* **22**, 34.
Zirin, H.: 1973, *Vistas in Astronomy*, in press (BBSO, No. 0111).
Zirin, H. and Lackner, R.: 1969, *Solar Phys.* **6**, 86.
Zirin, H., Pruss, G., and Vorpahl, J.: 1971, *Solar Phys.* **19**, 463.